



**HAL**  
open science

# Mechanobiology of muscle and myofibril morphogenesis

Nuno Miguel Luis, Frank Schnorrer

► **To cite this version:**

Nuno Miguel Luis, Frank Schnorrer. Mechanobiology of muscle and myofibril morphogenesis. *Cells & Development*, 2021, pp.203760. 10.1016/j.cdev.2021.203760 . hal-03471272

**HAL Id: hal-03471272**

**<https://hal.science/hal-03471272>**

Submitted on 8 Dec 2021

**HAL** is a multi-disciplinary open access archive for the deposit and dissemination of scientific research documents, whether they are published or not. The documents may come from teaching and research institutions in France or abroad, or from public or private research centers.

L'archive ouverte pluridisciplinaire **HAL**, est destinée au dépôt et à la diffusion de documents scientifiques de niveau recherche, publiés ou non, émanant des établissements d'enseignement et de recherche français ou étrangers, des laboratoires publics ou privés.

## Mechanobiology of muscle and myofibril morphogenesis

Nuno Miguel Luis<sup>1</sup> & Frank Schnorrer<sup>1</sup>

<sup>1</sup> Aix Marseille University, CNRS, IBDM, Turing Centre for Living Systems, 13288 Marseille,  
France

Correspondence should be addressed to:

[nuno.luis@univ-amu.fr](mailto:nuno.luis@univ-amu.fr)

[frank.schnorrer@univ-amu.fr](mailto:frank.schnorrer@univ-amu.fr)

keywords: muscle; sarcomere; biomechanics; mitochondria; *Drosophila*; titin;

## **Abstract**

**Muscles generate forces for animal locomotion. The contractile apparatus of muscles is the sarcomere, a highly regular array of large actin and myosin filaments linked by gigantic titin springs. During muscle development many sarcomeres assemble in series into long periodic myofibrils that mechanically connect the attached skeleton elements. Thus, ATP-driven myosin forces can power movement of the skeleton. Here we review muscle and myofibril morphogenesis, with a particular focus on their mechanobiology. We describe recent progress on the molecular structure of sarcomeres and their mechanical connections to the skeleton. We discuss current models predicting how tension coordinates the assembly of key sarcomeric components to periodic myofibrils that then further mature during development. This requires transcriptional feedback mechanisms that may help to coordinate myofibril assembly and maturation states with the transcriptional program. To fuel the varying energy demands of muscles we also discuss the close mechanical interactions of myofibrils with mitochondria and nuclei to optimally support powerful or enduring muscle fibers.**

## Highlights

- Update on the pseudo-crystalline structure of the sarcomere
- Molecularly detailing the development of force resistant muscle-tendon attachments
- Model for tension-driven myofibril self-assembly and myofibril maturation
- Mechanical coordination of muscle morphogenesis by transcriptional feedbacks
- Muscle-type specific mitochondrial and myofibril architectures



## Contents

### 1. The musculoskeletal system

*1.1 The sarcomere – a pseudo-crystalline force producing machine*

*1.2 Titin – a ruling and force sensing giant spring protein*

### 2. Muscle attachments

*2.1 Force-resistant muscle attachments: how to link a sarcomere to the skeleton*

*2.2 Quantifying molecular forces at muscle attachments*

### 3. Muscle and sarcomere morphogenesis

*3.1 Muscle-tendon attachment*

*3.2 Myofibril and sarcomere assembly*

*3.3 Myofibril and sarcomere maturation*

*3.4 Muscle fiber growth*

*3.5 Transcriptional dynamics recapitulates morphogenesis phases*

### 4. Morphogenesis coordination within a myofiber

### 5. Conclusions and perspectives

## 1. The musculoskeletal system

An average human individual synthesises per day about half its body weight in form of ATP to power basic body functions. Each ATP/ADP molecule is turned over about 1000 times per day<sup>1,2</sup>. An exercising athlete, such as a Tour de France cyclist, can consume up to 32 Mega Joule during a five-hour stage, more than five times the energy used during a regular day<sup>3</sup>. This enormous amount of energy is largely needed to fuel the myosin motor proteins of the muscles that produce the mechanical forces to power cyclists up the climbs. Even more impressive, flying animals power themselves into the air, with mosquitos beating their wings up to 1000 times per second giving rise to their well appreciated tone<sup>4</sup>.

For the efficient conversion of chemical energy into body movements it is critical that first, the energy is produced close to the consuming motors; second, the force generation of the many individual motor proteins is efficiently coordinated; and third, the force is converted into effective movements of the skeleton. If any of these conditions were not met, the muscles would run out of energy or largely produce heat instead of movement. Hence, the musculoskeletal system is a highly optimised biochemical apparatus that needs to form during animal development to match specific needs. In this review, we aim to cover the morphogenesis of muscles with a particular focus on the mechanobiology of its contractile machine, the sarcomere, the force transduction to the skeleton and lastly muscles' intracellular compartmentalisation optimised to fuel the molecular motors.

Skeletal muscles in vertebrates or body muscles in insects are large multinucleated cells, called muscle fibers, which can be tens of centimetres long in large vertebrates and are about 1 mm long in small fruit flies<sup>5,6</sup>. Both muscle fibers ends are connected via tendon cells to the skeleton, a bony endoskeleton in vertebrates or a chitin-based exoskeleton in insects<sup>5-7</sup>. The precise insertion sites of the tendons at the skeletal elements together with hinges placed between different skeletal elements ensure that shortening of the muscle fibers causes effective

1 movement of legs or wings (Figure 1A). Hence, the morphogenesis of skeleton, tendons and  
2 muscles must be precisely coordinated during animal development<sup>8-10</sup>.  
3  
4  
5

### 6 7 *1.1 The sarcomere – a pseudo-crystalline force producing machine*

8  
9 At the ‘heart’ of every muscle fiber is the muscles’ contractile machine, the sarcomere. We  
10 know since pioneering work in the 1950ies that sarcomeres contract by a sliding mechanism  
11  
12  
13  
14<sup>11,12</sup>: thick bipolar myosin filaments, which are anchored at the sarcomeric M-band, pull on  
15 precisely organised parallel actin filaments, which are cross-linked at the sarcomeric Z-discs  
16 bordering the sarcomere (Figure 1B). Hence, by pulling on the actin filaments the myosin  
17  
18  
19  
20  
21  
22  
23  
24  
25  
26  
27  
28  
29  
30  
31  
32  
33  
34  
35  
36  
37  
38  
39  
40  
41  
42  
43  
44  
45  
46  
47  
48  
49  
50  
51  
52  
53  
54  
55  
56  
57  
58  
59  
60  
61  
62  
63  
64  
65

How is sarcomere length controlled? Actin and myosin filaments are stably connected  
by the largest human protein, titin, whose N-terminus is bound to  $\alpha$ -actinin at the Z-disc,  
whereas its C-terminus is located in the middle of the sarcomere embedded into the M-band  
(Figure 1B)<sup>14-17</sup>. Thus, titin is thought to serve as the ruler of the sarcomere determining its  
resting length, usually between 2 and 3  $\mu\text{m}$  in vertebrate muscle, depending on species and  
muscle type<sup>18-20</sup>.

Mature sarcomeres display a pseudo-crystalline order of their components. In  
particular, insect flight muscles are so regular that structural changes of contracting sarcomeres  
can be observed in the flying animal (during tethered flight) using X-ray diffraction<sup>21,22</sup>. This  
provided molecular evidence for the long-proposed stretch activation mechanism of insect  
flight<sup>23-25</sup>: stretch-induced myosin and possibly troponin deformations are needed for efficient  
binding of myosin motors to actin and thus to trigger fast oscillations of the antagonistic insect  
flight muscle pairs. This showed that sarcomeres are excellently suited for structural studies.  
Understanding the mature structure is the first step to understand how a sarcomere is built

1 during muscle development. Hence, we briefly summarise our current structural knowledge of  
2 the sarcomeric parts.  
3

4 **Z-discs:** despite its high regularity, resolving the native molecular structure of a  
5 sarcomere in muscles is still an ambitious goal, especially for protein dense and complex  
6 regions such as the Z-disc. However, significant progress has been made using X-ray  
7 crystallography of purified sarcomeric proteins that are present in the Z-disc, in particular its  
8 core member  $\alpha$ -actinin.  $\alpha$ -actinin contains an N-terminal actin binding domain, four central  
9 spectrin repeats and a C-terminal calmodulin-like domain. The latter binds to the N-terminal  
10 Z-repeats of titin and thus anchors titin directly at the Z-disc<sup>26,27</sup>. The high-resolution structure  
11 of the purified 200 kDa  $\alpha$ -actinin dimer provides a first basis for how this interaction may be  
12 regulated<sup>28,29</sup>: the structure revealed that PIP2 binding to  $\alpha$ -actinin's actin binding domain can  
13 release the calmodulin-like domain and hence make it available for titin binding<sup>28</sup>, as has been  
14 suggested by biochemical experiments<sup>30,31</sup>. Interestingly, mutations in  $\alpha$ -actinin that alter the  
15 titin interaction dynamics show defects in sarcomere formation in cell culture models<sup>28</sup>.  
16 Furthermore, the structural model of the anti-parallel  $\alpha$ -actinin dimer places the two actin  
17 filaments bound to it 23 nm apart, which is in almost perfect agreement with the 24 nm spacing  
18 of tetragonal Z-disc lattice found in native mammalian muscle by electron microscopy<sup>32</sup>. The  
19 structure further suggested that the bound actin filaments have rotational freedom with respect  
20 to the stiff  $\alpha$ -actinin rod, in analogy to a 'pivot and rod' structure, resulting in some structural  
21 flexibility of Z-disc<sup>29</sup>.  
22  
23  
24  
25  
26  
27  
28  
29  
30  
31  
32  
33  
34  
35  
36  
37  
38  
39  
40  
41  
42  
43  
44  
45  
46  
47  
48

49 The flexibility of the Z-disc can also be affected by its thickness, which varies  
50 depending on mammalian muscle type from 30 nm in fast fibers up to 100 nm in slow and  
51 cardiac fibers<sup>33</sup> and about 80 nm in insect flight muscles<sup>34</sup> strongly suggesting that multiple  
52 columns of crosslinked  $\alpha$ -actinin exist at the Z-disc (Figure 1B). Differences might be  
53 regulated by alternatively spliced titin isoforms containing variable number of Z-repeats<sup>29,35</sup>  
54  
55  
56  
57  
58  
59  
60  
61  
62  
63  
64  
65

1 and thus more  $\alpha$ -actinin binding sites or by presence of alternatively spliced Zasp (Z-disc  
2 Alternatively Spliced Protein) isoforms, part of the Alp/Enigma conserved family of  
3 scaffolding proteins, which can also interact with  $\alpha$ -actinin via its PDZ domain and were  
4 recently proposed to regulate the diameter of the Z-disc in insect muscles by an oligomerisation  
5 mechanism<sup>36</sup>. The native sarcomeric Z-disc also houses a proposed titin cross-linker telethonin  
6  
7  
8  
9  
10  
11  
12  
13  
14  
15  
16  
17  
18  
19  
20  
21  
22  
23  
24  
25  
26  
27  
28  
29  
30  
31  
32  
33  
34  
35  
36  
37  
38  
39  
40  
41  
42  
43  
44  
45  
46  
47  
48  
49  
50  
51  
52  
53  
54  
55  
56  
57  
58  
59  
60  
61  
62  
63  
64  
65

**Thin and thick filaments:** to investigate the architecture of thin and thick filaments as well as their regulated interaction structural studies using purified *in vitro* assembled subcomplexes have been very insightful. Cryo-electron microscopy has revealed the architecture of a F-actin–tropomyosin complex with and without a myosin head demonstrating how a tropomyosin shift enables myosin binding and how the myosin motor head interacts with the actin filament at the molecular level<sup>41-43</sup>. This provided a molecular model for how myosin forces are transduced to actin filaments in a regulated way in the sarcomere<sup>43</sup>. Thus, *in vitro* assembled structures of sarcomeric components can teach us about the likely *in vivo* arrangement of these components and will be key structural models to resolve the native sarcomere structure *in situ*<sup>44</sup>.

Taking advantage of the stability of sarcomere subcomplexes, *Drosophila* or *Lethocerus* flight muscle thick filaments have been isolated and analysed with cryo-electron tomography. Although not yet at atomic resolution, these studies visualised the long  $\alpha$ -helices of the myosin rods in their native environment and revealed how their parallel arranged tails are packed together: interestingly, the individual myosin tails run in an angle from the main direction of the thick filament, forming a layered or ‘ribbon-like’ super-structure slowly

1 wrapping around the thick filament axis <sup>45,46</sup>, similar to what has been proposed in the 1970ies

2 47

3  
4  
5 **M-band:** thick filament associated proteins, such as myosin binding protein C in  
6 vertebrates and myofilin or paramyosin in insect muscles, have not yet been fully resolved  
7 structurally. Similarly, the native structure of the key M-band components myomesin and  
8 obscurin are unknown. Myomesin forms C-terminal dimers with a suggested role to bridge  
9 between neighbouring thick filaments (Figure 1B) <sup>48,49</sup>. Interestingly, these myomesin dimers  
10 can be elastically stretched to more than double their length at forces around 30 pN that might  
11 be physiologically relevant during muscle contractions <sup>50</sup>. This is consistent with a proposed  
12 strain absorber function of myomesin at the M-band <sup>51</sup>. Myomesin is not present in insect  
13 muscles, however the large M-band protein obscurin (Unc-89) is conserved and required for  
14 M-band alignment in *Drosophila* flight muscles and *C. elegans* body muscles <sup>52-55</sup>. In  
15 mammalian muscle, obscurin binds to the C-terminus of titin as well as to myomesin and hence  
16 also localises to the M-band <sup>56-58</sup>. However, its role in sarcomerogenesis is unclear <sup>59</sup>.

17  
18  
19  
20  
21  
22  
23  
24  
25  
26  
27  
28  
29  
30  
31  
32  
33  
34 **Towards a first native sarcomere structure:** one recent approach towards resolving  
35 the native sarcomere nanostructure with all its components included was to perform cryo-  
36 focused ion beam-milling electron tomography on intact myofibrils isolated from mouse  
37 muscles. This revealed that  $\alpha$ -actinin dimers indeed cross-link anti-parallel actin filaments at  
38 native Z-discs <sup>60</sup>. It also provided a structural explanation of how actin filaments, helped by  
39 stabilising myosin cross-bridges, transition from their square-like symmetry at Z-discs to their  
40 hexagonal pattern in the A-band <sup>60</sup>. Future cryo-electron tomography studies should reveal  
41 further details of the native sarcomere nanostructure.

## 52 53 54 55 56 *1.2 Titin – a ruling and force sensing giant spring protein*

1 Titin is a key sarcomeric protein that in vertebrate muscle spans across half the sarcomere, with  
2 its N-terminus anchored at the Z-disc and its C-terminus embedded into the M-band. Its  
3  
4 function in muscle architecture as well as muscle mechanics has been excellently reviewed  
5  
6 recently <sup>61,62</sup>, thus, we focus here on some recent highlights providing overwhelming evidence  
7  
8 that titin does rule sarcomere length and that titin can be a force sensing spring.  
9  
10

11  
12 In mammalian skeletal or cardiac muscle, the myosin filament is 1.6  $\mu\text{m}$  long (30 nm  
13 diameter) <sup>63</sup>, consisting of about 300 muscle myosin II hexamers <sup>64-66</sup>. The A-band part of titin  
14  
15 consists of immunoglobulin (Ig) and fibronectin type 3 (Fn3) domain super-repeats that are  
16  
17 constitutively present in the classical long titin isoforms in all muscle types. Hence, the length  
18  
19 of these titin super-repeats was long suggested as a blueprint, or ruler, for the observed  
20  
21 stereotypic length of the thick filaments. Indeed, genetic reduction of the number of A-band  
22  
23 Ig-Fn3 titin super-repeats caused the expected reduction of thick filament length and as  
24  
25 consequence, these muscle fibers produce lower forces <sup>67</sup>. This provided direct evidence for  
26  
27 titin's role regulating thick filament length and thus A-band length of mammalian sarcomeres  
28  
29 (Figure 1C).  
30  
31  
32  
33  
34  
35

36  
37 If titin determines A-band length, which is constant during the sarcomere contraction  
38  
39 cycle, how about the I-band, whose length changes during contraction? The I-band part of titin  
40  
41 consists of a long series of Ig domains followed by an unstructured region rich in amino acids  
42  
43 proline, glutamic acid, valine and lysine (PEVK), which are known to function as an elastic  
44  
45 spring, extending and relaxing during sarcomere contraction cycles (Figure 1D) <sup>61,62,68</sup>.  
46  
47

48  
49 The length of the I-band part of titin is muscle-type specific and regulated largely by  
50  
51 alternative splicing, with the general correlation that long Ig series and flexible PEVK  
52  
53 containing titin isoforms result in long I-bands present in mammalian skeletal and insect body  
54  
55 muscles, whereas short titin I-band versions, containing few PEVK and less Ig domains, result  
56  
57 in short I-bands present in cardiac muscle or insect flight muscle <sup>61,69-71</sup>. As a result, cardiac or  
58  
59  
60  
61  
62  
63  
64  
65

1 flight muscles are much stiffer compared to skeletal muscle. This has important functional  
2 consequences, particularly prominent during mammalian heart beat or insect flight, both of  
3 which are regulated with a large stretch-activation component <sup>72,73</sup>. It is hypothesized that this  
4 stretch-activation (or length-dependent activation) requires the shorter and stiffer titin isoform  
5 to communicate stretch effectively to fully activate actin and myosin filaments for the next  
6 contraction cycle <sup>22,61,69,74</sup>.

7  
8  
9  
10  
11  
12  
13  
14 Nevertheless, these findings provided only indirect evidence that titin rules I-band  
15 length in muscles. Direct evidence was recently obtained by deleting a large part of titin's  
16 PEVK spring using mouse genetics. Interestingly, the resulting mice are viable, grow to normal  
17 size and have muscles with normal lengths, however, their sarcomeric I-bands are shorter,  
18 resulting in shorter sarcomeres (Figure 1C). As a consequence, the muscle fiber assembles  
19 more sarcomeres, likely by a tension-driven assembly mechanism (see section 3), to  
20 mechanically connect over the same length, forming a muscle fiber that is stiffer compared to  
21 wild type <sup>75</sup>. Surprisingly, these mice are performing equally well, at least in a simple running  
22 wheel assay <sup>75</sup>. This provided direct evidence that titin's flexible PEVK spring determines the  
23 length of the I-band and largely contributes to the elasticity and thus passive stiffness of the  
24 muscle fiber.

25  
26  
27  
28  
29  
30  
31  
32  
33  
34  
35  
36  
37  
38  
39  
40  
41 The elastic properties of the PEVK spring have been investigated using single molecule  
42 atomic force microscopy or optical tweezers on native titin or recombinantly expressed protein  
43 domains. This established that titin's PEVK sequence acts as a perfectly elastic spring at low  
44 pico-newton forces <sup>76-78</sup>, which are likely present on endogenous titin during sarcomere  
45 contraction-relaxation cycles *in vivo* (Figure 1D) <sup>17,79</sup>. However, initial pulling experiments  
46 suggested that much larger forces are needed to unfold titin's Ig domains <sup>77,80,81</sup>, questioning  
47 whether or not Ig domain unfolding may also happen during normal muscle contraction cycles.  
48 Interestingly, recent experiments pulling with magnetic tweezers on recombinantly expressed  
49  
50  
51  
52  
53  
54  
55  
56  
57  
58  
59  
60  
61  
62  
63  
64  
65



1 titin fragments showed that at least some titin Ig domains can already unfold and refold at  
2 forces around 10 pN<sup>82-84</sup>, which are likely present across individual titin molecules *in vivo*.  
3  
4 Refolding of Ig and PEVK domains can produce work and hence can contribute to force  
5 produced by a contracting sarcomere, in addition to the active myosin force (Figure 1D),  
6  
7 similarly to how a stretched spring stores elastic energy released when recoiling back to normal  
8  
9 its normal length<sup>82-84</sup>. It has been estimated that the refolding of titin's domains under load can  
10  
11 produce a work of about 40zJ per titin molecule<sup>84</sup>, which is comparable to the work produced  
12  
13 by one myosin motor cycle<sup>85</sup>. On the other hand, during muscle contraction cycles an  
14  
15 antagonistic muscle is usually stretched (not shown in Figure 1A), hence work is needed to  
16  
17 unfold PEVK and potentially Ig domains in the antagonistic muscle. Thus, the net contribution  
18  
19 of titin refolding to the active contractile force *in vivo* remains unclear.  
20  
21  
22  
23  
24  
25

26  
27 The range of forces present across a titin molecule in a native sarcomere has not yet  
28  
29 been determined. However, the recent introduction of a TEV protease cleavage site at the end  
30  
31 of the I-band part of mouse titin provided very strong evidence that titin does transduce forces  
32  
33 *in vivo*: cleaving titin in the I-band in permeabilised muscles *ex vivo* resulted in quick  
34  
35 dislocation of the myosin filaments and a splitting of the sarcomeric A-band, when muscle  
36  
37 contractions were induced<sup>86</sup>. Passive tension in these titin cleaved muscles is reduced by more  
38  
39 than 50%<sup>84,86</sup>. This demonstrated the key role of titin as an elastic buffer for the forces exerted  
40  
41 by myosin during muscle contraction by stably linking the Z-disc to the sarcomeric M-band.  
42  
43 Hence, titin is in the perfect position to sense the molecular forces present in a native sarcomere.  
44  
45  
46  
47  
48  
49  
50

## 51 **2. Muscle attachments**

### 52 *2.1 Force-resistant muscle attachments: how to link a sarcomere to the skeleton*

53  
54 As discussed above, effective body movements require not only effective force production in  
55  
56 the muscle fibers but also an efficient force transduction to the skeleton (Figure 1A). As bone  
57  
58  
59  
60  
61  
62  
63  
64  
65

1 or chitinous skeleton is generally hard, whereas muscle tissue is soft, this generates high  
2 demands for the material interfaces connecting the two tissues<sup>87</sup>. Nature solved this challenge  
3  
4 by placing tendon cells between muscles and skeleton, hence allowing for a more graded  
5  
6 transition between these different cell types with such different stiffness. In mammals, tendons  
7  
8 cells are surrounded by a graded extracellular matrix (ECM) containing triple helical collagen  
9  
10 I, as well as collagen II, together with increasing amounts of mineralised calcium phosphate  
11  
12 (apatite) closer to the bone surface<sup>5,88</sup>. In *Drosophila*, which only possess a single tendon cell  
13  
14 layer between the cuticle and the flight muscles (Figure 2A), the ECM facing the apical surface  
15  
16 of the tendons is formed by the gigantic, fiber forming protein Dumpy<sup>89-91</sup>, whereas its basal  
17  
18 side connecting the tendons with the muscle fibers is an integrin-based adhesion with tigrin,  
19  
20 laminins and possibly collagen IV as ECM components<sup>92</sup>. Thus, a material with a graded  
21  
22 stiffness is used to stably anchor soft muscles to the stiff skeleton.  
23  
24  
25  
26  
27  
28

29 The terminal sarcomere of each myofibril faces a similar challenge as it needs to stably  
30  
31 attach to the ECM, which links muscle cells to tendons. One strategy to increase the anchoring  
32  
33 stability is to increase the surface contact. Hence *Drosophila* flight muscles and also the  
34  
35 intercalated discs of cardiomyocytes linking neighbouring sarcomeres, contain extensively  
36  
37 folded membrane indentations that largely increase the interaction surface (Figure 2A)<sup>93,94</sup>.  
38  
39 Recently, super-resolution microscopy of flight muscle-tendon attachments revealed an  
40  
41 interesting layered organisation between the ECM and the terminal Z-disc of a myofibril<sup>94</sup>:  
42  
43 proximal to the membrane is the integrin signalling layer with an extended integrin adaptor  
44  
45 talin. Talin, in its extended conformation, recruits vinculin in a force dependent manner<sup>95,96</sup>.  
46  
47 Additionally, focal adhesion kinase (Fak) is present in the signalling layer (Figure 2A). This is  
48  
49 followed by an actin-rich layer with Arp2/3, filamin, Zasp and  $\alpha$ -actinin nucleating and cross-  
50  
51 linking actin into a dense but not well-ordered actin network that links to the terminal Z-disc  
52  
53 of the myofibril (Figure 2A)<sup>94</sup>. This complex organisation can enable various feedback  
54  
55  
56  
57  
58  
59  
60  
61  
62  
63  
64  
65

1 mechanisms to optimally adjust adhesion in response to the high force produced by muscle  
2 fibers.  
3

## 4 5 6 7 2.2 *Quantifying molecular forces at muscle attachments* 8

9 Integrin adhesions are very well characterised force transducing macro-molecular assemblies  
10  
11 <sup>97</sup>. One key component linking integrin tails to the actin cytoskeleton and hence mediating the  
12 force transduction between integrins and the cytoskeleton is the integrin adaptor talin <sup>98,99</sup>.  
13  
14 Talin binds with its head to the beta-integrin tail and with its rod to the actin cytoskeleton,  
15  
16 which upon the application of force opens to expose vinculin binding sites that in turn enable  
17  
18 more actin filaments to pull on talin and induce focal adhesion growth <sup>100,101</sup>. Hence, talin is at  
19  
20 a key location to sense the range of forces present at muscle attachment sites.  
21  
22  
23  
24  
25

26  
27 Recent developments of genetically encodable FRET-based molecular force sensors  
28  
29 made it possible to quantify molecular forces across proteins in cell culture or *in vivo* <sup>102</sup>. These  
30  
31 sensors contain a small mechanosensitive peptide between the FRET pair with a calibrated  
32  
33 force range between 2 to 11 pN <sup>102</sup>. The application of high forces unfolds the elastic peptide,  
34  
35 resulting in low FRET values (Figure 2B).  
36  
37  
38

39 Such molecular tension sensors have been inserted into the endogenous talin gene in  
40  
41 *Drosophila* to quantify forces across talin at flight muscle attachments <sup>103</sup>. Surprisingly, it was  
42  
43 found that in mature adult flight muscles at rest, only a small amount of the talin molecules is  
44  
45 under force. However, if talin amounts are reduced to about half, the flight muscle-tendon  
46  
47 junction mechanically ruptures. This suggests that recruiting a large pool of talin molecules to  
48  
49 mature attachments is an efficient way to share peak forces likely present during active flight  
50  
51 muscle contractions <sup>103</sup>. We can wonder how recruitment of such a large pool of talin  
52  
53 molecules, and all other sarcomeric components, is coordinated temporally and spatially during  
54  
55  
56  
57  
58  
59  
60  
61  
62  
63  
64  
65

1 muscle development in a regulated way? We are addressing this question in the following  
2 section.  
3  
4  
5  
6

### 7 **3. Muscle and sarcomere morphogenesis**

8  
9 Muscle development with a focus on muscle patterning or myoblast fusion has been excellently  
10 reviewed recently <sup>104-109</sup>. Here we focus on recent advances in mechanical aspects of muscle  
11 morphogenesis and sarcomere development in particular. We use the well-studied *Drosophila*  
12 indirect flight muscles as one model system to elaborate common concepts of muscle and  
13 sarcomere morphogenesis as well as to highlight specific differences to mammalian skeletal  
14 muscle development.  
15  
16  
17  
18  
19  
20  
21  
22  
23  
24  
25

#### 26 *3.1 Muscle-tendon attachment*

27  
28 Each of the *Drosophila* indirect flight muscles is built during pupal stages by fusion of several  
29 hundred myoblasts to large syncytial myotubes <sup>110,111</sup>. These myotubes elongate at both ends  
30 towards their future attachment sites to which they establish a force-resistant integrin  
31 dependent attachment at 24 h after puparium formation (24 h APF, Figure 3A) <sup>112,113</sup>. During  
32 myotube elongation, myoblast fusion is largely restricted to the lateral membranes and absent  
33 from the dynamic leading edges, which are extending towards the tendons <sup>113,114</sup>. A similar  
34 myotube elongation process towards developing tendon attachments initiates myotube  
35 development in other *Drosophila* muscle types and also in a wide range of vertebrate muscles  
36 <sup>8,115-118</sup>. Hence, elongation and attachment are common principles of early muscle  
37 morphogenesis that define the long axis of each muscle fiber. This axis also determines the  
38 future muscle contraction axis, which will not be changed anymore during later steps of muscle  
39 morphogenesis.  
40  
41  
42  
43  
44  
45  
46  
47  
48  
49  
50  
51  
52  
53  
54  
55  
56  
57  
58  
59  
60  
61  
62  
63  
64  
65

1 During myotube-tendon attachment, mechanical tension is built-up within the  
2 myotendinous system: initially, tissue tension is low and only small amounts of integrin, talin  
3 and other integrin associated proteins are present at myotube attachment sites. When tissue  
4 tension increases, large amounts of integrin and talin are recruited and attachments mature over  
5 the next 6 h (until 30 h APF) <sup>103,113</sup>. This tension increase causes the compaction of the flight  
6 muscle myotube and its transition into an immature myofiber at 30 h APF (Figure 3A),  
7 coinciding with the self-assembling of immature myofibrils that connect both attachments (see  
8 section 3.2) <sup>103,113,119</sup>. At this stage, attachments have matured enough to be able to resist the  
9 first active muscle twitchings <sup>120</sup>. This indicates that attachment maturation and myofibril  
10 assembly must be coordinated during development.  
11  
12  
13  
14  
15  
16  
17  
18  
19  
20  
21  
22  
23

24 How is attachment maturation triggered molecularly and how is it coordinated with  
25 tissue tension increase? A first step to understand this coordination was undertaken by  
26 quantifying molecular forces across talin at developing muscle attachments (see Figure 2B).  
27 Interestingly, molecular tension across each talin molecule is larger at the early stages when  
28 few talin molecules are present and gradually reduces when more molecules are recruited <sup>103</sup>.  
29 This suggests that force dependent recruitment of talin is one important mechanism of  
30 attachment maturation. Integrin associated proteins are also recruited in a force dependent  
31 manner in *Drosophila* embryonic muscles. In particular the more peripheral members vinculin  
32 and paxillin strongly depend on muscle myosin activity, and thus muscle twitching, for  
33 effective recruitment and maturation of embryonic muscle attachments <sup>121</sup>. This fits with the  
34 interpretation that force-induced stretching of the talin rod will enable vinculin recruitment <sup>95</sup>.  
35 This is also well established in mammalian cells <sup>98,101,102</sup> and in beating cardiomyocytes, in the  
36 latter the oscillating forces across talin have even been directly quantified *in vitro* <sup>122</sup>. Together,  
37 this suggests that the tension dependent recruitment of large amounts of integrin complex  
38 proteins provides a buffer for peak forces produced by muscle contractions. This mechanical  
39  
40  
41  
42  
43  
44  
45  
46  
47  
48  
49  
50  
51  
52  
53  
54  
55  
56  
57  
58  
59  
60  
61  
62  
63  
64  
65

1 feedback mechanism coordinates muscle-tendon attachment morphogenesis with formation of  
2 contractile sarcomeres and prevents a fatal rupture of attachments.  
3  
4  
5

### 6 7 3.2 Myofibril and sarcomere assembly 8

9 Developing myofibers are very long cells connecting two skeletal elements. However, each  
10 contractile sarcomere is only a few micrometres long (see Figure 1). How do myofibers manage  
11 to assemble the correct number of sarcomeres into long myofibrils to bridge the long distance,  
12 maintaining but not exceeding the correct tension level in each of its sarcomeric components?  
13  
14 One possible mechanism to solve this ‘dimension problem’ is suggested by the tension-driven  
15 myofibril self-organisation hypothesis<sup>68,113</sup>. This hypothesis, postulated in *Drosophila*, is  
16 likely to also apply to mammalian muscles<sup>123-126</sup>. It suggests that mechanical tension is  
17 coordinating the assembly of many smaller molecular complexes into higher order periodic  
18 structures throughout the entire large muscle fiber. These long continuous and periodic  
19 myofibrils mechanically bridge both ends of the entire muscle (Figure 3B). Live imaging has  
20 shown that a periodic pattern in myofibrils indeed appears simultaneously over long distances  
21 in *Drosophila* muscles as well as in cultured cardiomyocytes, suggesting a self-organisation  
22 mechanism<sup>113,117,123,124</sup>. How could such a phenomenon work molecularly?  
23  
24  
25  
26  
27  
28  
29  
30  
31  
32  
33  
34  
35  
36  
37  
38  
39  
40

41 In early stage myotubes, actomyosin is organised in a polar network along the long  
42 muscle axis possessing a rather low molecular order without distinct myofibrils<sup>127,128</sup>. As most  
43 major sarcomeric components such as titin, muscle myosin or troponin are absent at this stage  
44  
45  
46  
47  
48  
49  
50  
51  
52  
53  
54  
55  
56  
57  
58  
59  
60  
61  
62  
63  
64  
65

66 However, non-muscle myosin assembles into rather short, up to 300 nm long, bipolar filaments  
67  
68  
69  
70  
71  
72  
73  
74  
75  
76  
77  
78  
79  
80  
81  
82  
83  
84  
85  
86  
87  
88  
89  
90  
91  
92  
93  
94  
95  
96  
97  
98  
99  
100

101  
102  
103  
104  
105  
106  
107  
108  
109  
110  
111  
112  
113  
114  
115  
116  
117  
118  
119  
120  
121  
122  
123  
124  
125  
126  
127  
128  
129  
130  
131  
132  
133  
134  
135  
136  
137  
138  
139  
140  
141  
142  
143  
144  
145  
146  
147  
148  
149  
150  
151  
152  
153  
154  
155  
156  
157  
158  
159  
160  
161  
162  
163  
164  
165

166  
167  
168  
169  
170  
171  
172  
173  
174  
175  
176  
177  
178  
179  
180  
181  
182  
183  
184  
185  
186  
187  
188  
189  
190  
191  
192  
193  
194  
195  
196  
197  
198  
199  
200

201  
202  
203  
204  
205  
206  
207  
208  
209  
210  
211  
212  
213  
214  
215  
216  
217  
218  
219  
220  
221  
222  
223  
224  
225  
226  
227  
228  
229  
230  
231  
232  
233  
234  
235  
236  
237  
238  
239  
240  
241  
242  
243  
244  
245  
246  
247  
248  
249  
250  
251  
252  
253  
254  
255  
256  
257  
258  
259  
260  
261  
262  
263  
264  
265

266  
267  
268  
269  
270  
271  
272  
273  
274  
275  
276  
277  
278  
279  
280  
281  
282  
283  
284  
285  
286  
287  
288  
289  
290  
291  
292  
293  
294  
295  
296  
297  
298  
299  
300

301  
302  
303  
304  
305  
306  
307  
308  
309  
310  
311  
312  
313  
314  
315  
316  
317  
318  
319  
320  
321  
322  
323  
324  
325  
326  
327  
328  
329  
330  
331  
332  
333  
334  
335  
336  
337  
338  
339  
340  
341  
342  
343  
344  
345  
346  
347  
348  
349  
350  
351  
352  
353  
354  
355  
356  
357  
358  
359  
360  
361  
362  
363  
364  
365

366  
367  
368  
369  
370  
371  
372  
373  
374  
375  
376  
377  
378  
379  
380  
381  
382  
383  
384  
385  
386  
387  
388  
389  
390  
391  
392  
393  
394  
395  
396  
397  
398  
399  
400

401  
402  
403  
404  
405  
406  
407  
408  
409  
410  
411  
412  
413  
414  
415  
416  
417  
418  
419  
420  
421  
422  
423  
424  
425  
426  
427  
428  
429  
430  
431  
432  
433  
434  
435  
436  
437  
438  
439  
440  
441  
442  
443  
444  
445  
446  
447  
448  
449  
450  
451  
452  
453  
454  
455  
456  
457  
458  
459  
460  
461  
462  
463  
464  
465

466  
467  
468  
469  
470  
471  
472  
473  
474  
475  
476  
477  
478  
479  
480  
481  
482  
483  
484  
485  
486  
487  
488  
489  
490  
491  
492  
493  
494  
495  
496  
497  
498  
499  
500

501  
502  
503  
504  
505  
506  
507  
508  
509  
510  
511  
512  
513  
514  
515  
516  
517  
518  
519  
520  
521  
522  
523  
524  
525  
526  
527  
528  
529  
530  
531  
532  
533  
534  
535  
536  
537  
538  
539  
540  
541  
542  
543  
544  
545  
546  
547  
548  
549  
550  
551  
552  
553  
554  
555  
556  
557  
558  
559  
560  
561  
562  
563  
564  
565

566  
567  
568  
569  
570  
571  
572  
573  
574  
575  
576  
577  
578  
579  
580  
581  
582  
583  
584  
585  
586  
587  
588  
589  
590  
591  
592  
593  
594  
595  
596  
597  
598  
599  
600

601  
602  
603  
604  
605  
606  
607  
608  
609  
610  
611  
612  
613  
614  
615  
616  
617  
618  
619  
620  
621  
622  
623  
624  
625  
626  
627  
628  
629  
630  
631  
632  
633  
634  
635  
636  
637  
638  
639  
640  
641  
642  
643  
644  
645  
646  
647  
648  
649  
650  
651  
652  
653  
654  
655  
656  
657  
658  
659  
660  
661  
662  
663  
664  
665

666  
667  
668  
669  
670  
671  
672  
673  
674  
675  
676  
677  
678  
679  
680  
681  
682  
683  
684  
685  
686  
687  
688  
689  
690  
691  
692  
693  
694  
695  
696  
697  
698  
699  
700

701  
702  
703  
704  
705  
706  
707  
708  
709  
710  
711  
712  
713  
714  
715  
716  
717  
718  
719  
720  
721  
722  
723  
724  
725  
726  
727  
728  
729  
730  
731  
732  
733  
734  
735  
736  
737  
738  
739  
740  
741  
742  
743  
744  
745  
746  
747  
748  
749  
750  
751  
752  
753  
754  
755  
756  
757  
758  
759  
760  
761  
762  
763  
764  
765

766  
767  
768  
769  
770  
771  
772  
773  
774  
775  
776  
777  
778  
779  
780  
781  
782  
783  
784  
785  
786  
787  
788  
789  
790  
791  
792  
793  
794  
795  
796  
797  
798  
799  
800

801  
802  
803  
804  
805  
806  
807  
808  
809  
810  
811  
812  
813  
814  
815  
816  
817  
818  
819  
820  
821  
822  
823  
824  
825  
826  
827  
828  
829  
830  
831  
832  
833  
834  
835  
836  
837  
838  
839  
840  
841  
842  
843  
844  
845  
846  
847  
848  
849  
850  
851  
852  
853  
854  
855  
856  
857  
858  
859  
860  
861  
862  
863  
864  
865

866  
867  
868  
869  
870  
871  
872  
873  
874  
875  
876  
877  
878  
879  
880  
881  
882  
883  
884  
885  
886  
887  
888  
889  
890  
891  
892  
893  
894  
895  
896  
897  
898  
899  
900

901  
902  
903  
904  
905  
906  
907  
908  
909  
910  
911  
912  
913  
914  
915  
916  
917  
918  
919  
920  
921  
922  
923  
924  
925  
926  
927  
928  
929  
930  
931  
932  
933  
934  
935  
936  
937  
938  
939  
940  
941  
942  
943  
944  
945  
946  
947  
948  
949  
950  
951  
952  
953  
954  
955  
956  
957  
958  
959  
960  
961  
962  
963  
964  
965

966  
967  
968  
969  
970  
971  
972  
973  
974  
975  
976  
977  
978  
979  
980  
981  
982  
983  
984  
985  
986  
987  
988  
989  
990  
991  
992  
993  
994  
995  
996  
997  
998  
999  
1000

1 myosin assembles several hundred hexamers (composed of 2 heavy chains, 2 essential and 2  
2 regulatory light chains) into 1.6  $\mu\text{m}$  long filaments in mammalian muscle or into more than  
3  
4 3.0  $\mu\text{m}$  long bipolar filaments in insect muscles<sup>65</sup>. Hence with the onset of muscle myosin  
5  
6 expression, non-muscle myosin filaments are either replaced with muscle myosin ones, as  
7  
8 suggested by the pre-myofibril model<sup>130,131</sup>, or the simple increase in muscle myosin levels  
9  
10 results in the dominant incorporation of muscle myosin into periodic immature myofibrils that  
11  
12 span the entire muscle fiber length (Figure 3B). These myofibrils are chains of immature  
13  
14 sarcomeres, containing periodic cross-linked actin filaments of increasing molecular order as  
15  
16 development progresses<sup>128</sup>, as well as titin,  $\alpha$ -actinin, obscurin, Zasp and likely other  
17  
18 components<sup>54,113,132,133</sup>. Thus, not only actin and myosin but additional, possibly preassembled,  
19  
20 protein complexes are organising into these continuous immature myofibrils<sup>134-136</sup>. They may  
21  
22 use mechanical tension as a compass to orient themselves properly to assemble the correct  
23  
24 number of immature sarcomeres within each myofibril. The better the assembly, the higher the  
25  
26 active force that myosin can produce by pulling on ordered actin filaments (Figure 3A, B)<sup>68</sup>.  
27  
28  
29  
30  
31  
32  
33  
34  
35

### 36 3.3 Myofibril and sarcomere maturation

37 Immature sarcomeres are contractile, but they are not yet fully adapted to the specific needs of  
38  
39 the respective muscle type, be it a slow or fast mammalian fiber or an insect flight muscle fiber.  
40  
41 Sarcomere maturation is particularly well illustrated in *Drosophila* flight muscles, which  
42  
43 simultaneously assemble all their 2000 myofibrils per muscle fiber that mature synchronously  
44  
45 without addition of new myofibrils until the adult stage (Figure 3A, B)<sup>120</sup>. During these  
46  
47 maturation steps sarcomere length grows from about 2  $\mu\text{m}$  to 3.4  $\mu\text{m}$  and myofibril diameter  
48  
49 progressively increases to reach about 1.5  $\mu\text{m}$ <sup>120,133,137,138</sup>. How is such a defined sarcomere  
50  
51 growth achieved?  
52  
53  
54  
55  
56  
57  
58  
59  
60  
61  
62  
63  
64  
65

1  
2  
3  
4  
5  
6  
7  
8  
9  
10  
11  
12  
13  
14  
15  
16  
17  
18  
19  
20  
21  
22  
23  
24  
25  
26  
27  
28  
29  
30  
31  
32  
33  
34  
35  
36  
37  
38  
39  
40  
41  
42  
43  
44  
45  
46  
47  
48  
49  
50  
51  
52  
53  
54  
55  
56  
57  
58  
59  
60  
61  
62  
63  
64  
65

Although not understood in molecular detail, it is likely that the relative amounts and the specific sarcomeric protein isoforms present at any time point determine the precise sarcomere architecture during sarcomere maturation. Expression of muscle myosin heavy chain isoforms changes via a switch in alternative splicing in flight muscles<sup>137,139</sup> or via a transcriptional switch during mammalian muscle development from embryonic to fetal and finally to adult isoforms (Figure 3B)<sup>140</sup>. Actin filament length growth is controlled by the expression of capping proteins like Tmod and Sals<sup>141-143</sup>, as well as actin nucleators, including the formin family member Fhos or the short nebulin homolog Lasp during flight muscle sarcomere maturation<sup>144,145</sup>. Similar proteins are needed to control actin filament length in mammalian muscle development, such as the formin homolog FHOD3<sup>146</sup>, and in particular the gigantic protein nebulin whose proposed function as actin filament ruler has been reviewed in detail<sup>62,147-149</sup>.

A particularly impressive way of how myofibril diameter can be regulated was recently proposed for flight muscles: the three distinct Zasp genes (*Zasp52*, *Zasp66* and *Zasp67*) encode either short Zasp isoforms only containing a PDZ-domain and the Zasp-motif (ZM) domain or long isoforms with additional 1 to 4 LIM domains<sup>132,138</sup>. Interestingly, these Zasp proteins are core components of the Z-discs and can form aggregates by an interaction of their ZM domain with one of the LIM domains, whereas their PDZ domain interacts with  $\alpha$ -actinin<sup>132,150</sup>. Consequently, Zasp isoforms with one or more LIM domains promote ZASP complex growth and hence Z-disc growth, whereas short isoforms, lacking any LIM domain, block further growth. Strikingly, expression of ‘growing’ isoforms is high during myofibril maturation and diameter growth, whereas ‘blocking’ isoforms are upregulated only very late to terminate growth. Consistently, ‘growing’ isoforms are found located more centrally in the Z-discs, compared to blocking isoforms<sup>138</sup>. These findings underscore the importance to coordinate



transcriptional regulation with sarcomere morphogenesis to form functional sarcomeres (see sections 3.4 and 3.5).

### 3.4 Muscle fiber growth

In mammalian embryonic and adult muscles, muscle fiber growth is largely driven by continuous myoblast fusion to existing fibers<sup>151,152</sup> resulting in a fiber volume per nucleus correlation termed the myonuclear domain size<sup>153</sup>. Careful volume measurements in *Drosophila* larval muscles also revealed a striking correlation of muscle fiber volume with nuclear volume<sup>154</sup>. This correlation is maintained during the rapid insulin-induced growth of the *Drosophila* larval muscles: instead of additional myoblasts fusing, the larval muscle nuclei undergo several rounds of DNA endo-replication to produce very large nuclei, with up to 64 copies of each chromosome<sup>154,155</sup>. Interestingly, the number of endo-replication cycles appears to be regulated mechanically via the LINC complex, which links the lamin meshwork below the nuclear membrane to the sarcomere and microtubule cytoskeleton<sup>156</sup>. This provides a possible mechanical feedback mechanism to control nuclear endo-replication cycles during larval muscle fiber growth.

Further support for a significant mechanical input to the muscle nuclei is given by their specific positions. In *Drosophila* larval muscles, nuclei are initially transported by microtubules to clusters located close to the fiber ends<sup>157,158</sup>. When sarcomeres have assembled and the fibers grow, the nuclei are redistributed and equally spaced along the fiber length, suggesting that a force-balance mechanism equally positions them per muscle volume<sup>154,159</sup>. Furthermore, the larval nuclei are pushed to the surface of the larval muscles by the growing myofibrils and microtubules<sup>160</sup>. Very similarly, nuclei in mature mammalian muscle fibers are also equally spaced along the fiber axis and are pushed to the fiber surface by the maturing and contracting myofibrils<sup>161,162</sup>. In developing flight muscles, most nuclei are located centrally at

1  
2  
3  
4  
5  
6  
7  
8  
9  
10  
11  
12  
13  
14  
15  
16  
17  
18  
19  
20  
21  
22  
23  
24  
25  
26  
27  
28  
29  
30  
31  
32  
33  
34  
35  
36  
37  
38  
39  
40  
41  
42  
43  
44  
45  
46  
47  
48  
49  
50  
51  
52  
53  
54  
55  
56  
57  
58  
59  
60  
61  
62  
63  
64  
65

24 h APF before myofibrils are forming (Figure 3A). Upon myofibril assembly, they relocate and fill the space between the growing myofibril bundles<sup>163</sup>. As a consequence, all nuclei adopt an elongated shape along the myofibril axis. Together, this strongly suggests that myofibrils impact nuclear shape and mechanics during muscle fiber growth.

*Drosophila* flight muscles grow tremendously after myoblast fusion has ceased, increasing their volume more than ten-fold in three days (Figure 3A)<sup>163</sup>. Since their final number of myofibrils is already determined at 30 h APF, flight muscle length growth coincides with the addition of new sarcomeres to each existing myofibril, while their increase in diameter causes muscle diameter growth (Figure 3A, see section 3.3). Additionally, the mitochondrial content increases enormously (see section 4)<sup>164</sup>. It is unknown if flight muscle nuclei undergo endoreplication, however a classical tissue growth pathway was recently shown to be essential during postmitotic flight muscle growth. Loss of the transcriptional regulator Yorkie (YAP, TAZ in mammals) or gain of the Hippo or Warts kinases, which are negatively regulating Yorkie, result in a block of flight muscle fiber growth<sup>163</sup>. While these fibers finish myoblast fusion normally, they assemble fewer myofibrils, which then fail to mature, resulting in a dramatic muscle growth defect<sup>163</sup>. The Hippo pathway has a well described key mechanosensory function at the epithelial cell cortex regulating stretch-dependent epithelial cell growth<sup>165-168</sup>. However, how can the Hippo pathway sense stretch in muscle fibers to induce muscle growth?

Interestingly, the classical upstream Hippo regulators Expanded, Merlin or Kibra that are involved in sensing stretch at the epithelial cell cortex do not seem to be required in flight muscles. Instead, the STRIPAK phosphatase complex controls Hippo activity. Slmap, one member of the STRIPAK complex binds to Dlg5, both of which are present in internal membranes forming the future T-tubules in proximity to the assembling myofibrils<sup>163</sup>. Thus, it was speculated that in analogy to sensing stretch at the epithelial cell membrane, mechanical

1 stretch might be sensed at these internal muscle membranes to control Hippo kinase activity  
2 before and after myofibril assembly. Consequently, expression of key sarcomeric components  
3  
4 is reduced upon loss of Yorkie, suggesting that mechanics and possibly myofibril assembly  
5  
6 status may feedback on the transcriptional state of the developing muscle fiber to induce its  
7  
8 further growth <sup>163</sup>.  
9  
10

### 11 *3.5 Transcriptional dynamics recapitulates morphogenesis phases*

12  
13  
14 As highlighted above, muscle fiber development can be divided into multiple phases such as  
15  
16 early muscle fate choice, myoblast fusion, myotube elongation and attachment, myofibril  
17  
18 assembly and maturation, as well as muscle fiber growth. Flight muscles are a suitable model  
19  
20 to study how transcriptional dynamics may impact the different phases, as their development  
21  
22 is largely homogenous. A systematic transcriptomic time-course covering flight muscle  
23  
24 development from myoblast stage in third instar larvae to mature adult flight muscles revealed  
25  
26 that the different morphogenesis phases are indeed preceded by important transcriptional  
27  
28 transitions <sup>120</sup>. As expected, genes implicated in patterning and cell division dominate the early  
29  
30 phase when myoblasts are dividing and their future muscle fate is determined (Figure 3C).  
31  
32 Then cell adhesion and muscle attachment genes become upregulated, fitting with the next  
33  
34 morphogenesis step, the attachment of the myotubes to tendons. At this stage, the expression  
35  
36 of sarcomeric genes is still very low, showing that only after successful myotube attachment  
37  
38 the expression of the key sarcomeric genes is initiated enabling myofibril assembly (Figure  
39  
40 3C) <sup>120</sup>. As discussed above, one signalling pathway that may react to mechanical input is the  
41  
42 Hippo pathway needed for effective sarcomere gene expression <sup>163</sup>. However, as Hippo  
43  
44 signalling appears to be particularly important only in flight muscles it remains to be seen how  
45  
46 other muscles regulate this important transition.  
47  
48  
49  
50  
51  
52  
53  
54  
55  
56  
57  
58  
59  
60  
61  
62  
63  
64  
65

1 A subset of sarcomeric genes or gene isoforms, including the titin-like protein  
2 Stretchin-MLCK, are only expressed at late stages during sarcomere maturation, once the  
3 general sarcomere scaffold is built <sup>120</sup>. How could this late boost of sarcomere expression be  
4 controlled? General muscle-specific regulators such as Mef2 are needed throughout flight  
5 muscle development <sup>169</sup> and also the flight muscle identity transcription factor Spalt is needed  
6 both at the beginning to set up muscle fate and for the efficient boost at late stages <sup>120</sup>.  
7 Interestingly, E2F, known for its key role during the cell cycle in many cell types <sup>170</sup>, is  
8 dispensable for myoblast proliferation or fusion in *Drosophila* muscles and only needed at late  
9 stages for myofibril assembly and, in particular, for myofibril maturation and fiber growth <sup>171</sup>.  
10 Together with the results from the Hippo pathway, this demonstrates that key transcriptional  
11 regulators controlling cell cycle and growth in dividing tissue can be repurposed allowing  
12 postmitotic muscle cell growth.  
13  
14  
15  
16  
17  
18  
19  
20  
21  
22  
23  
24  
25  
26  
27

28  
29 It is important to note that flight muscle morphogenesis is not only controlled at the  
30 transcriptional level, but alternative splicing is also critical in many different muscle types <sup>70,172</sup>.  
31 In flight muscles, the splicing regulator Bruno (arrest), a CELF family member, is  
32 transcriptionally induced by Spalt at the stage of myofibril assembly. However, Bruno is  
33 largely needed to instruct flight muscle specific splicing during sarcomere maturation, for  
34 example enabling splicing of the correct Stretchin-MLCK isoform. Consequently, *bruno*  
35 mutant flight muscles show severe myofibril maturation defects <sup>139,173</sup>. This further illustrates  
36 that transcriptional dynamics must be well synchronised with the morphogenesis phases of the  
37 muscle fibers.  
38  
39  
40  
41  
42  
43  
44  
45  
46  
47  
48  
49  
50  
51  
52

#### 53 **4. Morphogenesis coordination within a myofiber**

54 As illustrated above, maturing muscle fibers are very densely packed cells with a defined  
55 tension axis. While it is well established that the mechanical properties of the extracellular  
56  
57  
58  
59  
60  
61  
62  
63  
64  
65

1 environment can directly impact cell fate, including muscle fate choice <sup>174,175</sup>, it is less clear  
2 how tension and mechanical interactions between various intracellular organelles and  
3 molecular machines are sensed and coordinated <sup>176</sup>. For muscle fibers, it particularly matters to  
4 correctly partition their myofibrils, their mitochondria and their nuclei in a fiber-type specific  
5 way to efficiently support insect flight or long-distance running (Figure 4).  
6  
7  
8  
9  
10

11 The increasing crowdedness of differentiating muscle fibers strongly restricts diffusion  
12 of mRNAs <sup>177</sup>. Thus, in mature muscle fibers most mRNAs undergo microtubule-based  
13 transport when exiting the nucleus before they are translated <sup>177</sup>. Interestingly, mature  
14 cardiomyocytes and skeletal muscle fibers show a strong enrichment of ribosomes close to  
15 their sarcomeric Z-discs, at which not only mRNAs coding for sarcomeric proteins, but most  
16 mRNAs appear to be translated. <sup>177-179</sup>. If proteins are mostly synthesised at these ‘translation  
17 hubs’ <sup>177</sup>, how do they efficiently reach their destinations in the nuclei, mitochondria or muscle  
18 attachments, as protein diffusion in dense myofibers is restricted <sup>180</sup>? This is a particular  
19 challenge for the most abundant organelle inside muscle fibers, the mitochondria, which import  
20 most of their proteins from the cytoplasm <sup>181</sup>. The answer might be resolved by live imaging  
21 of individual protein dynamics in muscle in the future.  
22  
23  
24  
25  
26  
27  
28  
29  
30  
31  
32  
33  
34  
35  
36  
37  
38

39 Three-dimensional electron microscopy techniques <sup>182</sup> are now allowing to reconstruct  
40 the detailed 3D morphology of muscle fibers revealing precise mitochondria shapes and their  
41 relation to the myofibrils. Interestingly, in mammalian muscles mitochondria form elongated  
42 networks whose locations and shapes depend on the muscle fiber type. In glycolytic fibers,  
43 elongated mitochondria are largely oriented perpendicular to the contraction axis, whereas in  
44 oxidative slow fibers mitochondria form a grid like network and in cardiomyocytes the network  
45 is exclusively oriented in the direction of the myofibrils <sup>183</sup>. This leads to an increased  
46 proximity between mitochondria and myosin filaments in myofibrils of oxidative and cardiac  
47  
48  
49  
50  
51  
52  
53  
54  
55  
56  
57  
58  
59  
60  
61  
62  
63  
64  
65

1 myofibers compared to glycolytic ones and hence increase the efficiency of ATP delivery for  
2 their function <sup>183</sup>.  
3

4  
5 Oxidative fibers and in particular cardiomyocytes contain up to 35% of mitochondria  
6 per total muscle volume <sup>183,184</sup>, making it likely that mitochondria are not only providing the  
7 myofibers with energy but also influence them mechanically. Indeed, in mammalian skeletal  
8 muscles these mitochondrial networks form thin extensions or ‘nanotunnels’ close to the  
9 aligned myofibrils at their sarcomeric I-bands, in proximity to the sarcoplasmic reticulum and  
10 the T-tubule network <sup>183,185,186</sup>. Some of these tunnels are connecting two distant larger  
11 mitochondria generating an extensive network (Figure 4, right panel) <sup>186</sup>. Interestingly, also in  
12 *Drosophila* muscles the mitochondrial shapes and networks strongly depend on muscle fiber-  
13 types: cross-striated leg muscles contain complex shaped mitochondrial networks with similar  
14 mitochondrial nanochannels along their sarcomeric I-bands as in mammalian muscle fibers <sup>164</sup>.  
15  
16 In contrast, flight muscle mitochondria are elongated along each of the individual myofibrils  
17 adopting ellipsoid-like shapes that ensheath myofibrils and isolate them from their  
18 neighbouring myofibrils (Figure 4, left panel) <sup>164</sup>. This creates a large mitochondria-myofibril  
19 interface that will enable an optimised ATP/ADP exchange to feed the high energy demands  
20 during flight. Mitochondria-myofibril proximity is emphasized by the finding that myofibrils  
21 are pushing the mitochondria into the elongated shapes since releasing the pressure or  
22 disassembling the myofibrils results in a rounding of the mitochondria <sup>164</sup>. How can such close  
23 ties arise in a coordinated way during muscle development?  
24  
25

26  
27 Recent studies of developing *Drosophila* flight muscles showed that in myotubes,  
28 before myofibrils assembly, mitochondria are thin elongated tubes and assemble to local  
29 networks largely excluded from the actin filament bundles <sup>164</sup>. Concomitantly with the  
30 assembly of the immature myofibrils (see Figure 3B), mitochondria intercalate between them  
31 and insulate each myofibril from its neighbours <sup>164,187</sup>. When myofibrils start to mature and  
32  
33  
34  
35  
36  
37  
38  
39  
40  
41  
42  
43  
44  
45  
46  
47  
48  
49  
50  
51  
52  
53  
54  
55  
56  
57  
58  
59  
60  
61  
62  
63  
64  
65

1 grow in diameter, mitochondria also dramatically increase in volume and grow until they are  
2 pushed from the myofibrils into ellipse shapes (Figure 4, left panel) <sup>164</sup>. At the same time,  
3 expression of mitochondrial genes is strongly boosted (Figure 3C) <sup>120,188</sup> and mitochondria  
4 dramatically increase their cristae density <sup>128,187</sup>, which are invaginations of the internal  
5 mitochondria membranes that house the electron transport chain components <sup>189</sup>. The higher  
6 the cristae surface, the higher the respiration capacity of the mitochondria, a feature particularly  
7 associated with oxidative fibers <sup>190</sup>. Similarly dynamic mitochondria remodelling has been  
8 observed in mammalian cardiomyocytes shortly after birth when myofibrils grow in size <sup>191</sup>.  
9 This demonstrates that mitochondria morphogenesis is intimately coordinated with myofibril  
10 morphogenesis.  
11  
12  
13  
14  
15  
16  
17  
18  
19  
20  
21  
22  
23

24 One possible mechanism how to coordinate morphogenesis of both organelles has  
25 recently been suggested from studies of developing flight muscles. Changing the mitochondrial  
26 fusion and fission dynamics during development in the direction of increased fusion and hence  
27 larger mitochondrial clusters prevents the intercalation of the mitochondria between the  
28 developing myofibrils <sup>164</sup>. Interestingly, this intercalation block causes the alignment of the  
29 otherwise individualised flight muscle myofibrils changing them to a cross-striated  
30 morphology normally found in leg muscles. Strikingly, the transcriptional status of these flight  
31 muscles also changes and sarcomeric protein isoforms that are normally flight muscle specific  
32 are reduced, whereas leg muscle specific proteins are boosted. This suggested a mechanical  
33 feedback mechanism from the mitochondria and myofibrils back to the nuclei adapting their  
34 transcriptional program <sup>164</sup>. As the nuclei are in close proximity to and pushed by the myofibrils  
35 to their fiber-type specific positions (Figure 4 and see section 3), it is conceivable that the nuclei  
36 themselves, possibly using the LINC complex in the nuclear membrane, sense the mechanical  
37 changes and adapt their transcriptional program accordingly <sup>156,192</sup>. Appropriate mitochondrial  
38 fusion and fission dynamics are also needed during mammalian muscle and heart development  
39  
40  
41  
42  
43  
44  
45  
46  
47  
48  
49  
50  
51  
52  
53  
54  
55  
56  
57  
58  
59  
60  
61  
62  
63  
64  
65

193-195 leading us to speculate that similar mechanical feedback mechanisms may coordinate mitochondria with myofibril development in mammalian muscle.

## 5. Concluding remarks

Cellular mechanics controls the function and the development of most eukaryotic cell types and tissues, with a prime role in muscle and heart. The development of the muscle contractile machinery directly impacts the mechanical properties of muscle cells and hence feedbacks to coordinate its development with its surrounding tissues as well as with the other muscle cell organelles. We are just beginning to understand how such feedback mechanisms work molecularly to coordinate the formation of functional muscle cells. In the future, muscle and heart biology will continue to profit from novel high-resolution microscopy techniques, in particular electron tomography, to investigate the native muscle nanostructure and similarly from the *in vivo* application of live imaging tools that will allow to quantify individual protein dynamics and turnover rates as well as mechanical forces in developing muscle cells. Combining these technologies with genetic models and automated analysis tools will hopefully create the required synergism to reveal the nanostructure of the muscle and understand how biomechanical coordination between its components can assemble such beautiful contractile machines.

## Competing interests

The authors declare that no competing interests exist.

## Acknowledgements



1 We are grateful to Jerome Avellaneda for providing the electron microscopy image shown in  
2 Figure 2A and for Sandra Lemke for integrin attachment and talin tensor sensor schemes  
3 modified for Figure 2A and B. We thank Holger Knaut, Pierre Mangeol and Qiyao Mao for  
4 insightful comments on this review.  
5  
6  
7  
8  
9

## 10 **Funding**

11 This work was supported by the Centre National de la Recherche Scientifique (CNRS, N.M.L.,  
12 F.S.), the European Research Council under the European Union's Horizon 2020 Programme  
13 (ERC-2019-SyG 856118, F.S.), the excellence initiative Aix-Marseille University A\*MIDEX  
14 (ANR-11-IDEX-0001-02, F.S.), the French National Research Agency with ANR-ACHN  
15 MUSCLE-FORCES and ANR-18-CE45-0016-01 MITO-DYNAMICS (F.S.), the Human  
16 Frontiers Science Program (HFSP, RGP0052/2018, F.S.), the Bettencourt Foundation (F.S.),  
17 the France-BioImaging national research infrastructure (ANR-10-INBS-04-01) and the  
18 Investissements d'Avenir, French Government program managed by the French National  
19 Research Agency (ANR-16-CONV-0001) and from Excellence Initiative of Aix-Marseille  
20 University - A\*MIDEX (Turing Centre for Living Systems).  
21  
22  
23  
24  
25  
26  
27  
28  
29  
30  
31  
32  
33  
34  
35  
36  
37  
38

39 The funders had no role in study design, data collection and analysis, decision to publish, or  
40 preparation of the manuscript.  
41  
42  
43  
44  
45  
46  
47  
48  
49  
50  
51  
52  
53  
54  
55  
56  
57  
58  
59  
60  
61  
62  
63  
64  
65

## References

1. Neupane, P., Bhujju, S., Thapa, N. & Bhattarai, H. K. ATP Synthase: Structure, Function and Inhibition. *Biomol Concepts* **10**, 1–10 (2019).
2. Capaldi, R. A. & Aggeler, R. Mechanism of the F(1)F(0)-type ATP synthase, a biological rotary motor. *Trends in Biochemical Sciences* **27**, 154–160 (2002).
3. Saris, W. H., van Erp-Baart, M. A., Brouns, F., Westerterp, K. R. & Hoor, ten, F. Study on food intake and energy expenditure during extreme sustained exercise: the Tour de France. *Int J Sports Med* **10 Suppl 1**, S26–31 (1989).
4. Arthur, B. J., Emr, K. S., Wyttenbach, R. A. & Hoy, R. R. Mosquito (*Aedes aegypti*) flight tones: frequency, harmonicity, spherical spreading, and phase relationships. *J Acoust Soc Am* **135**, 933–941 (2014).
5. Zelzer, E., Blitz, E., Killian, M. L. & Thomopoulos, S. Tendon-to-bone attachment: from development to maturity. *Birth Defects Res C Embryo Today* **102**, 101–112 (2014).
6. Moussian, B. Chitin: Structure, Chemistry and Biology. *Adv. Exp. Med. Biol.* **1142**, 5–18 (2019).
7. Sidor, C. & Schnorrer, F. Mechanobiology: Forging a strong matrix at tendons. *Curr Biol* **31**, R347–R350 (2021).
8. Schnorrer, F. & Dickson, B. J. Muscle building; mechanisms of myotube guidance and attachment site selection. *Developmental Cell* **7**, 9–20 (2004).
9. Schweitzer, R., Zelzer, E. & Volk, T. Connecting muscles to tendons: tendons and musculoskeletal development in flies and vertebrates. *Development* **137**, 2807–2817 (2010).
10. Felsenthal, N. & Zelzer, E. Mechanical regulation of musculoskeletal system development. *Development* **144**, 4271–4283 (2017).
11. Huxley, A. F. & Niedergerke, R. Structural changes in muscle during contraction; interference microscopy of living muscle fibres. **173**, 971–973 (1954).
12. Huxley, H. & Hanson, J. Changes in the cross-striations of muscle during contraction and stretch and their structural interpretation. *Nature* **173**, 973–976 (1954).
13. Huxley, H. E. Memories of early work on muscle contraction and regulation in the 1950's and 1960's. *Biochemical and Biophysical Research Communications* **369**, 34–42 (2008).
14. Fürst, D. O., Osborn, M., Nave, R. & Weber, K. The organization of titin filaments in the half-sarcomere revealed by monoclonal antibodies in immunoelectron microscopy: a map of ten nonrepetitive epitopes starting at the Z line extends close to the M line. *Journal of Cell Biology* **106**, 1563–1572 (1988).
15. Linke, W. A. *et al.* Towards a molecular understanding of the elasticity of titin. *Journal of Molecular Biology* **261**, 62–71 (1996).
16. Maruyama, K., Natori, R. & Nonomura, Y. New elastic protein from muscle. *Nature* **262**, 58–60 (1976).
17. Gautel, M. & Goulding, D. A molecular map of titin/connectin elasticity reveals two different mechanisms acting in series. *FEBS letters* **385**, 11–14 (1996).
18. Tskhovrebova, L. & Trinick, J. Titin: properties and family relationships. *Nature Reviews Molecular Cell Biology* **4**, 679–689 (2003).
19. Llewellyn, M. E., Barretto, R. P. J., Delp, S. L. & Schnitzer, M. J. Minimally invasive high-speed imaging of sarcomere contractile dynamics in mice and humans. *Nature* **454**, 784–788 (2008).

20. Ehler, E. & Gautel, M. The sarcomere and sarcomerogenesis. *Adv. Exp. Med. Biol.* **642**, 1–14 (2008).
21. Dickinson, M., Bekyarova, T., Gore, D. & Maughan, D. Molecular dynamics of cyclically contracting insect flight muscle in vivo. *Nature* **433**, 330–334 (2005).
22. Iwamoto, H. & Yagi, N. The molecular trigger for high-speed wing beats in a bee. *Science* **341**, 1243–1246 (2013).
23. Pringle, J. W. The Bidder Lecture - The evolution of fibrillar muscle in insects. *J Exp Biol* **94**, 1–14 (1981).
24. Josephson, R. K., Malamud, J. G. & Stokes, D. R. Asynchronous muscle: a primer. *J Exp Biol* **203**, 2713–2722 (2000).
25. Agianian, B. *et al.* A troponin switch that regulates muscle contraction by stretch instead of calcium. *The EMBO Journal* **23**, 772–779 (2004).
26. Young, P., Ferguson, C., Bañuelos, S. & Gautel, M. Molecular structure of the sarcomeric Z-disk: two types of titin interactions lead to an asymmetrical sorting of alpha-actinin. *The EMBO Journal* **17**, 1614–1624 (1998).
27. Atkinson, R. A. *et al.* Ca<sup>2+</sup>-independent binding of an EF-hand domain to a novel motif in the alpha-actinin-titin complex. *Nat Struct Biol* **8**, 853–857 (2001).
28. Ribeiro, E. de A. *et al.* The structure and regulation of human muscle  $\alpha$ -actinin. *CELL* **159**, 1447–1460 (2014).
29. Gautel, M. & Djinović-Carugo, K. The sarcomeric cytoskeleton: from molecules to motion. *Journal of Experimental Biology* **219**, 135–145 (2016).
30. Fukami, K. *et al.* Requirement of phosphatidylinositol 4,5-bisphosphate for alpha-actinin function. *Nature* **359**, 150–152 (1992).
31. Young, P. & Gautel, M. The interaction of titin and alpha-actinin is controlled by a phospholipid-regulated intramolecular pseudoligand mechanism. *The EMBO Journal* **19**, 6331–6340 (2000).
32. Goldstein, M. A., Schroeter, J. P. & Sass, R. L. The Z lattice in canine cardiac muscle. *Journal of Cell Biology* **83**, 187–204 (1979).
33. Luther, P. K. The vertebrate muscle Z-disc: sarcomere anchor for structure and signalling. *J Muscle Res Cell Motil* **30**, 171–185 (2009).
34. Szikora, S. *et al.* Nanoscopy reveals the layered organization of the sarcomeric H-zone and I-band complexes. *The Journal of Cell Biology* **219**, (2020).
35. Gautel, M., Goulding, D., Bullard, B., Weber, K. & Fürst, D. O. The central Z-disk region of titin is assembled from a novel repeat in variable copy numbers. *Journal of Cell Science* **109 ( Pt 11)**, 2747–2754 (1996).
36. González-Morales, N., Holenka, T. K. & Schöck, F. Filamin actin-binding and titin-binding fulfill distinct functions in Z-disc cohesion. *PLoS Genetics* **13**, e1006880 (2017).
37. Zou, P. *et al.* Palindromic assembly of the giant muscle protein titin in the sarcomeric Z-disk. *Nature* **439**, 229–233 (2006).
38. Narita, A., Takeda, S., Yamashita, A. & Maéda, Y. Structural basis of actin filament capping at the barbed-end: a cryo-electron microscopy study. *The EMBO Journal* **25**, 5626–5633 (2006).
39. van der Ven, P. F. *et al.* Characterization of muscle filamin isoforms suggests a possible role of gamma-filamin/ABP-L in sarcomeric Z-disc formation. *Cell Motil. Cytoskeleton* **45**, 149–162 (2000).
40. Liao, K. A., González-Morales, N. & Schöck, F. Zasp52, a Core Z-disc Protein in Drosophila Indirect Flight Muscles, Interacts with  $\alpha$ -Actinin via an Extended PDZ Domain. *PLoS Genetics* **12**, e1006400 (2016).

- 1 41. Behrmann, E. *et al.* Structure of the rigor actin-tropomyosin-myosin complex. *CELL*  
2 **150**, 327–338 (2012).
- 3 42. Ecken, von der, J. *et al.* Structure of the F-actin--tropomyosin complex. *Nature* **519**,  
4 114–117 (2015).
- 5 43. Ecken, von der, J., Heissler, S. M., Pathan-Chhatbar, S., Manstein, D. J. & Raunser,  
6 S. Cryo-EM structure of a human cytoplasmic actomyosin complex at near-atomic  
7 resolution. *Nature* **534**, 724–728 (2016).
- 8 44. Taylor, K. A., Rahmani, H., Edwards, R. J. & Reedy, M. K. Insights into Actin-  
9 Myosin Interactions within Muscle from 3D Electron Microscopy. *Int J Mol Sci* **20**,  
10 (2019).
- 11 45. Hu, Z., Taylor, D. W., Reedy, M. K., Edwards, R. J. & Taylor, K. A. Structure of  
12 myosin filaments from relaxed *Lethocerus* flight muscle by cryo-EM at 6 Å  
13 resolution. *Sci Adv* **2**, e1600058 (2016).
- 14 46. Daneshparvar, N. *et al.* CryoEM structure of *Drosophila* flight muscle thick filaments  
15 at 7 Å resolution. *Life Sci. Alliance* **3**, (2020).
- 16 47. Squire, J. M. General model of myosin filament structure. II. Myosin filaments and  
17 cross-bridge interactions in vertebrate striated and insect flight muscles. *Journal of*  
18 *Molecular Biology* **72**, 125–138 (1972).
- 19 48. Lange, S. *et al.* Dimerisation of myomesin: implications for the structure of the  
20 sarcomeric M-band. *Journal of Molecular Biology* **345**, 289–298 (2005).
- 21 49. Pinotsis, N., Lange, S., Perriard, J.-C., Svergun, D. I. & Wilmanns, M. Molecular  
22 basis of the C-terminal tail-to-tail assembly of the sarcomeric filament protein  
23 myomesin. *The EMBO Journal* **27**, 253–264 (2008).
- 24 50. Pinotsis, N. *et al.* Superhelical architecture of the myosin filament-linking protein  
25 myomesin with unusual elastic properties. *PLoS Biol* **10**, e1001261 (2012).
- 26 51. Berkemeier, F. *et al.* Fast-folding alpha-helices as reversible strain absorbers in the  
27 muscle protein myomesin. *Proceedings of the National Academy of Sciences* **108**,  
28 14139–14144 (2011).
- 29 52. Qadota, H., Blangy, A., Xiong, G. & Benian, G. M. The DH-PH region of the giant  
30 protein UNC-89 activates RHO-1 GTPase in *Caenorhabditis elegans* body wall  
31 muscle. *Journal of Molecular Biology* **383**, 747–752 (2008).
- 32 53. Benian, G. M. & Mayans, O. Titin and obscurin: giants holding hands and discovery  
33 of a new Ig domain subset. *Journal of Molecular Biology* **427**, 707–714 (2015).
- 34 54. Katzemich, A. *et al.* The function of the M-line protein obscurin in controlling the  
35 symmetry of the sarcomere in the flight muscle of *Drosophila*. *Journal of Cell*  
36 *Science* **125**, 3367–3379 (2012).
- 37 55. Schnorrer, F. *et al.* Systematic genetic analysis of muscle morphogenesis and  
38 function in *Drosophila*. *Nature* **464**, 287–291 (2010).
- 39 56. Fukuzawa, A. *et al.* Interactions with titin and myomesin target obscurin and  
40 obscurin-like 1 to the M-band: implications for hereditary myopathies. *Journal of*  
41 *Cell Science* **121**, 1841–1851 (2008).
- 42 57. Sauer, F., Vahokoski, J., Song, Y.-H. & Wilmanns, M. Molecular basis of the head-  
43 to-tail assembly of giant muscle proteins obscurin-like 1 and titin. *EMBO Rep* **11**,  
44 534–540 (2010).
- 45 58. Pernigo, S. *et al.* The crystal structure of the human titin:obscurin complex reveals a  
46 conserved yet specific muscle M-band zipper module. *Journal of Molecular Biology*  
47 **427**, 718–736 (2015).
- 48 59. Blondelle, J. *et al.* Murine obscurin and Obsl1 have functionally redundant roles in  
49 sarcolemmal integrity, sarcoplasmic reticulum organization, and muscle metabolism.  
50 *Communications Biology* **2**, 178–13 (2019).
- 51
- 52
- 53
- 54
- 55
- 56
- 57
- 58
- 59
- 60
- 61
- 62
- 63
- 64
- 65

- 1 60. Wang, Z. *et al.* The molecular basis for sarcomere organization in vertebrate skeletal  
2 muscle. *CELL* **184**, 2135–2150.e13 (2021).
- 3 61. Linke, W. A. Titin Gene and Protein Functions in Passive and Active Muscle. *Annu.*  
4 *Rev. Physiol.* **80**, 389–411 (2018).
- 5 62. Tskhovrebova, L. & Trinick, J. in *Fibrous Proteins: Structures and Mechanisms* **82**,  
6 285–318 (Springer International Publishing, 2017).
- 7 63. Tskhovrebova, L., Bennett, P., Gautel, M. & Trinick, J. Titin ruler hypothesis not  
8 refuted. *Proceedings of the National Academy of Sciences* **112**, E1172 (2015).
- 9 64. Sosa, H., Popp, D., Ouyang, G. & Huxley, H. E. Ultrastructure of skeletal muscle  
10 fibers studied by a plunge quick freezing method: myofilament lengths. *Biophysj* **67**,  
11 283–292 (1994).
- 12 65. Dasbiswas, K., Hu, S., Schnorrer, F., Safran, S. A. & Bershadsky, A. D. Ordering of  
13 myosin II filaments driven by mechanical forces: experiments and theory. *Philos.*  
14 *Trans. R. Soc. Lond., B, Biol. Sci.* **373**, 20170114 (2018).
- 15 66. Gokhin, D. S. & Fowler, V. M. A two-segment model for thin filament architecture  
16 in skeletal muscle. *Nature Reviews Molecular Cell Biology* **14**, 113–119 (2013).
- 17 67. Tonino, P. *et al.* The giant protein titin regulates the length of the striated muscle  
18 thick filament. *Nature Communications* **8**, 1041 (2017).
- 19 68. Lemke, S. B. & Schnorrer, F. Mechanical forces during muscle development.  
20 *Mechanisms of Development* **144**, 92–101 (2017).
- 21 69. Burkart, C. *et al.* Modular proteins from the *Drosophila* sallimus (sls) gene and their  
22 expression in muscles with different extensibility. *Journal of Molecular Biology* **367**,  
23 953–969 (2007).
- 24 70. Spletter, M. L. & Schnorrer, F. Transcriptional regulation and alternative splicing  
25 cooperate in muscle fiber-type specification in flies and mammals. *Experimental Cell*  
26 *Research* **321**, 90–98 (2014).
- 27 71. Granzier, H. & Labeit, S. Structure-function relations of the giant elastic protein titin  
28 in striated and smooth muscle cells. *Muscle Nerve* **36**, 740–755 (2007).
- 29 72. Bullard, B. & Pastore, A. Regulating the contraction of insect flight muscle. *J Muscle*  
30 *Res Cell Motil* **32**, 303–313 (2011).
- 31 73. Shiels, H. A. & White, E. The Frank-Starling mechanism in vertebrate cardiac  
32 myocytes. *J Exp Biol* **211**, 2005–2013 (2008).
- 33 74. de Tombe, P. P. *et al.* Myofilament length dependent activation. *J. Mol. Cell.*  
34 *Cardiol.* **48**, 851–858 (2010).
- 35 75. Brynnel, A. *et al.* Downsizing the molecular spring of the giant protein titin reveals  
36 that skeletal muscle titin determines passive stiffness and drives longitudinal  
37 hypertrophy. *eLife* **7**, 1065 (2018).
- 38 76. Watanabe, K. *et al.* Molecular mechanics of cardiac titin's PEVK and N2B spring  
39 elements. *Journal of Biological Chemistry* **277**, 11549–11558 (2002).
- 40 77. Linke, W. A. *et al.* PEVK domain of titin: an entropic spring with actin-binding  
41 properties. *J. Struct. Biol.* **137**, 194–205 (2002).
- 42 78. Leake, M. C., Wilson, D., Gautel, M. & Simmons, R. M. The elasticity of single titin  
43 molecules using a two-bead optical tweezers assay. *Biophysj* **87**, 1112–1135 (2004).
- 44 79. Linke, W. A., Ivemeyer, M., Mundel, P., Stockmeier, M. R. & Kolmerer, B. Nature  
45 of PEVK-titin elasticity in skeletal muscle. *Proceedings of the National Academy of*  
46 *Sciences of the United States of America* **95**, 8052–8057 (1998).
- 47 80. Rief, M., Gautel, M., Oesterhelt, F., Fernandez, J. M. & Gaub, H. E. Reversible  
48 unfolding of individual titin immunoglobulin domains by AFM. *Science* **276**, 1109–  
49 1112 (1997).
- 50  
51  
52  
53  
54  
55  
56  
57  
58  
59  
60  
61  
62  
63  
64  
65

- 1  
2  
3  
4  
5  
6  
7  
8  
9  
10  
11  
12  
13  
14  
15  
16  
17  
18  
19  
20  
21  
22  
23  
24  
25  
26  
27  
28  
29  
30  
31  
32  
33  
34  
35  
36  
37  
38  
39  
40  
41  
42  
43  
44  
45  
46  
47  
48  
49  
50  
51  
52  
53  
54  
55  
56  
57  
58  
59  
60  
61  
62  
63  
64  
65
81. Kellermayer, M. S., Smith, S. B., Granzier, H. L. & Bustamante, C. Folding-unfolding transitions in single titin molecules characterized with laser tweezers. *Science* **276**, 1112–1116 (1997).
  82. Rivas-Pardo, J. A. *et al.* Work Done by Titin Protein Folding Assists Muscle Contraction. *CellReports* **14**, 1339–1347 (2016).
  83. Eckels, E. C., Haldar, S., Tapia-Rojo, R., Rivas-Pardo, J. A. & Fernandez, J. M. The Mechanical Power of Titin Folding. *CellReports* **27**, 1836–1847.e4 (2019).
  84. Rivas-Pardo, J. A. *et al.* A HaloTag-TEV genetic cassette for mechanical phenotyping of proteins from tissues. *Nature Communications* **11**, 2060–13 (2020).
  85. Piazzesi, G. *et al.* Skeletal muscle performance determined by modulation of number of myosin motors rather than motor force or stroke size. *CELL* **131**, 784–795 (2007).
  86. Li, Y. *et al.* Graded titin cleavage progressively reduces tension and uncovers the source of A-band stability in contracting muscle. *eLife* **9**, (2020).
  87. Paxton, J. Z. & Baar, K. *Current progress in enthesis repair: strategies for interfacial tissue engineering.* (2012). doi:10.4172/2161-0533.S1-003
  88. Genin, G. M. *et al.* Functional grading of mineral and collagen in the attachment of tendon to bone. *Biophysical journal* **97**, 976–985 (2009).
  89. Bökel, C., Prokop, A. & Brown, N. H. Papillote and Piopio: Drosophila ZP-domain proteins required for cell adhesion to the apical extracellular matrix and microtubule organization. *Journal of Cell Science* **118**, 633–642 (2005).
  90. Chu, W.-C. & Hayashi, S. Mechano-chemical enforcement of tendon apical ECM into nano-filaments during Drosophila flight muscle development. *Curr Biol* **31**, 1366–1378.e7 (2021).
  91. Sidor, C. & Schnorrer, F. Mechanobiology: Forging a strong matrix at tendons. *Curr Biol* **31**, R347–R350 (2021).
  92. Brown, N. H. *et al.* Integrins as mediators of morphogenesis in Drosophila. **223**, 1–16 (2000).
  93. Reedy, M. C. & Beall, C. Ultrastructure of Developing Flight Muscle in Drosophila. II. Formation of the Myotendon Junction. *Dev. Biol.* **160**, 466–479 (1993).
  94. Green, H. J., Griffiths, A. G., Yläne, J. & Brown, N. H. Novel functions for integrin-associated proteins revealed by analysis of myofibril attachment in Drosophila. *eLife* **7**, 197 (2018).
  95. Klapholz, B. & Brown, N. H. Talin - the master of integrin adhesions. *Journal of Cell Science* jcs.190991–12 (2017). doi:10.1242/jcs.190991
  96. Klapholz, B. *et al.* Alternative mechanisms for talin to mediate integrin function. *Curr Biol* **25**, 847–857 (2015).
  97. Sun, Z., Guo, S. S. & Fässler, R. Integrin-mediated mechanotransduction. *The Journal of Cell Biology* **215**, 445–456 (2016).
  98. Sun, Z., Costell, M. & Fässler, R. Integrin activation by talin, kindlin and mechanical forces. *Nature cell biology* **21**, 25–31 (2019).
  99. Moser, M., Legate, K. R., Zent, R. & Fassler, R. The Tail of Integrins, Talin, and Kindlins. *Science* **324**, 895–899 (2009).
  100. Grashoff, C. *et al.* Measuring mechanical tension across vinculin reveals regulation of focal adhesion dynamics. *Nature* **466**, 263–266 (2010).
  101. Elosegui-Artola, A. *et al.* Mechanical regulation of a molecular clutch defines force transmission and transduction in response to matrix rigidity. *Nature cell biology* **18**, 540–548 (2016).
  102. Fischer, L. S., Rangarajan, S., Sadhanasatish, T. & Grashoff, C. Molecular Force Measurement with Tension Sensors. *Annu Rev Biophys* (2021). doi:10.1146/annurev-biophys-101920-064756

- 1  
2  
3  
4  
5  
6  
7  
8  
9  
10  
11  
12  
13  
14  
15  
16  
17  
18  
19  
20  
21  
22  
23  
24  
25  
26  
27  
28  
29  
30  
31  
32  
33  
34  
35  
36  
37  
38  
39  
40  
41  
42  
43  
44  
45  
46  
47  
48  
49  
50  
51  
52  
53  
54  
55  
56  
57  
58  
59  
60  
61  
62  
63  
64  
65
103. Lemke, S. B., Weidemann, T., Cost, A.-L., Grashoff, C. & Schnorrer, F. A small proportion of Talin molecules transmit forces at developing muscle attachments in vivo. *PLoS Biol* **17**, e3000057 (2019).
  104. Schiaffino, S. & Reggiani, C. Fiber types in mammalian skeletal muscles. *Physiological Reviews* **91**, 1447–1531 (2011).
  105. Bothe, I. & Baylies, M. K. Drosophila myogenesis. *Curr Biol* **26**, R786–91 (2016).
  106. Gunage, R. D., Dhanyasi, N., Reichert, H. & VijayRaghavan, K. Drosophila adult muscle development and regeneration. *Semin. Cell Dev. Biol.* **72**, 56–66 (2017).
  107. Sampath, S. C., Sampath, S. C. & Millay, D. P. Myoblast fusion confusion: the resolution begins. *Skeletal Muscle* **8**, 3–10 (2018).
  108. Lee, D. M. & Chen, E. H. Drosophila Myoblast Fusion: Invasion and Resistance for the Ultimate Union. *Annu Rev Genet* **53**, 67–91 (2019).
  109. Poovathumkadavil, P. & Jagla, K. Genetic Control of Muscle Diversification and Homeostasis: Insights from Drosophila. *Cells* **9**, 1543 (2020).
  110. Fernandes, J., Bate, M. & VijayRaghavan, K. Development of the indirect flight muscles of Drosophila. *Development* **113**, 67–77 (1991).
  111. Mukherjee, P., Gildor, B., Shilo, B.-Z., VijayRaghavan, K. & Schejter, E. D. The actin nucleator WASp is required for myoblast fusion during adult Drosophila myogenesis. *Development* **138**, 2347–2357 (2011).
  112. Fernandes, J., Celniker, S. & VijayRaghavan, K. Development of the Indirect Flight Muscle Attachment Sites in Drosophila: Role of the PS Integrins and the stripe Gene. **176**, 166–184 (1996).
  113. Weitkunat, M., Kaya-Copur, A., Grill, S. W. & Schnorrer, F. Tension and force-resistant attachment are essential for myofibrillogenesis in Drosophila flight muscle. *Curr Biol* **24**, 705–716 (2014).
  114. Sarov, M. *et al.* A genome-wide resource for the analysis of protein localisation in Drosophila. *eLife* **5**, e12068 (2016).
  115. Kardon, G., Harfe, B. D. & Tabin, C. J. A Tcf4-positive mesodermal population provides a prepattern for vertebrate limb muscle patterning. *Developmental Cell* **5**, 937–944 (2003).
  116. Gros, J., Serralbo, O. & Marcelle, C. WNT11 acts as a directional cue to organize the elongation of early muscle fibres. *Nature* **457**, 589–593 (2009).
  117. Weitkunat, M., Brasse, M., Bausch, A. R. & Schnorrer, F. Mechanical tension and spontaneous muscle twitching precede the formation of cross-striated muscle in vivo. *Development* **144**, 1261–1272 (2017).
  118. Wood, A. J. & Currie, P. D. Development Aspects of Zebrafish Myotendinous Junction: a Model System for Understanding Muscle Basement Membrane Formation and Failure. 1–9 (2017). doi:10.1007/s40139-017-0140-z
  119. Vega-Macaya, F., Manieu, C., Valdivia, M., Mlodzik, M. & Olguin, P. Establishment of the Muscle-Tendon Junction During Thorax Morphogenesis in Drosophila Requires the Rho-Kinase. **204**, 1139–1149 (2016).
  120. Spletter, M. L. *et al.* A transcriptomics resource reveals a transcriptional transition during ordered sarcomere morphogenesis in flight muscle. *eLife* **7**, 1361 (2018).
  121. Bulgakova, N. A., Wellmann, J. & Brown, N. H. Diverse integrin adhesion stoichiometries caused by varied actomyosin activity. *Open Biol* **7**, (2017).
  122. Pandey, P. *et al.* Cardiomyocytes Sense Matrix Rigidity through a Combination of Muscle and Non-muscle Myosin Contractions. *Developmental Cell* **44**, 326–336.e3 (2018).

- 1  
2  
3  
4  
5  
6  
7  
8  
9  
10  
11  
12  
13  
14  
15  
16  
17  
18  
19  
20  
21  
22  
23  
24  
25  
26  
27  
28  
29  
30  
31  
32  
33  
34  
35  
36  
37  
38  
39  
40  
41  
42  
43  
44  
45  
46  
47  
48  
49  
50  
51  
52  
53  
54  
55  
56  
57  
58  
59  
60  
61  
62  
63  
64  
65
123. Chopra, A. *et al.* Force Generation via  $\beta$ -Cardiac Myosin, Titin, and  $\alpha$ -Actinin Drives Cardiac Sarcomere Assembly from Cell-Matrix Adhesions. *Developmental Cell* **44**, 87–96.e5 (2018).
  124. Fenix, A. M. *et al.* Muscle-specific stress fibers give rise to sarcomeres in cardiomyocytes. *eLife* **7**, 1111 (2018).
  125. Taneja, N., Neininger, A. C. & Burnette, D. T. Coupling to substrate adhesions drives the maturation of muscle stress fibers into myofibrils within cardiomyocytes. *Molecular Biology of the Cell* **31**, 1273–1288 (2020).
  126. Mao, Q. *et al.* Tension-driven multi-scale self-organisation in human iPSC-derived muscle fibers. *bioRxiv* 2021.10.24.465614 (2021).
  127. Reedy, M. C. & Beall, C. Ultrastructure of developing flight muscle in *Drosophila*. I. Assembly of myofibrils. *Dev. Biol.* **160**, 443–465 (1993).
  128. Loison, O. *et al.* Polarization-resolved microscopy reveals a muscle myosin motor-independent mechanism of molecular actin ordering during sarcomere maturation. *PLoS Biol* **16**, e2004718 (2018).
  129. Hu, S. *et al.* Long-range self-organization of cytoskeletal myosin II filament stacks. *Nature cell biology* **19**, 133–141 (2017).
  130. Rhee, D., Sanger, J. M. & Sanger, J. W. The premyofibril: evidence for its role in myofibrillogenesis. *Cell Motil. Cytoskeleton* **28**, 1–24 (1994).
  131. Sanger, J. W., Wang, J., Fan, Y., White, J. & Sanger, J. M. Assembly and dynamics of myofibrils. *Journal of Biomedicine and Biotechnology* **2010**, 858606 (2010).
  132. Katzemich, A., Liao, K. A., Czerniecki, S. & Schöck, F. Alp/Enigma family proteins cooperate in Z-disc formation and myofibril assembly. *PLoS Genetics* **9**, e1003342 (2013).
  133. Orfanos, Z. *et al.* Sallimus and the dynamics of sarcomere assembly in *Drosophila* flight muscles. *Journal of Molecular Biology* **427**, 2151–2158 (2015).
  134. Holtzer, H. *et al.* Independent assembly of 1.6 microns long bipolar MHC filaments and I-Z-I bodies. *Cell Struct Funct* **22**, 83–93 (1997).
  135. Ehler, E., Rothen, B. M., Hämmerle, S. P., Komiyama, M. & Perriard, J. C. Myofibrillogenesis in the developing chicken heart: assembly of Z-disk, M-line and the thick filaments. *Journal of Cell Science* **112 ( Pt 10)**, 1529–1539 (1999).
  136. Rui, Y., Rui, Y., Bai, J. & Perrimon, N. Sarcomere formation occurs by the assembly of multiple latent protein complexes. *PLoS Genetics* **6**, e1001208 (2010).
  137. Orfanos, Z. & Sparrow, J. C. Myosin isoform switching during assembly of the *Drosophila* flight muscle thick filament lattice. *Journal of Cell Science* **126**, 139–148 (2013).
  138. González-Morales, N. *et al.* Myofibril diameter is set by a finely tuned mechanism of protein oligomerization in *Drosophila*. *eLife* **8**, (2019).
  139. Spletter, M. L. *et al.* The RNA-binding protein Arrest (Bruno) regulates alternative splicing to enable myofibril maturation in *Drosophila* flight muscle. *EMBO Rep* **16**, 178–191 (2015).
  140. Schiaffino, S., Rossi, A. C., Smerdu, V., Leinwand, L. A. & Reggiani, C. Developmental myosins: expression patterns and functional significance. *Skeletal Muscle* **5**, 22–14 (2015).
  141. Mardahl-Dumesnil, M. & Fowler, V. M. Thin filaments elongate from their pointed ends during myofibril assembly in *Drosophila* indirect flight muscle. *Journal of Cell Biology* **155**, 1043–1053 (2001).
  142. Bai, J., Hartwig, J. H. & Perrimon, N. SALS, a WH2-domain-containing protein, promotes sarcomeric actin filament elongation from pointed ends during *Drosophila* muscle growth. *Developmental Cell* **13**, 828–842 (2007).



- 1  
2  
3  
4  
5  
6  
7  
8  
9  
10  
11  
12  
13  
14  
15  
16  
17  
18  
19  
20  
21  
22  
23  
24  
25  
26  
27  
28  
29  
30  
31  
32  
33  
34  
35  
36  
37  
38  
39  
40  
41  
42  
43  
44  
45  
46  
47  
48  
49  
50  
51  
52  
53  
54  
55  
56  
57  
58  
59  
60  
61  
62  
63  
64  
65
143. Gokhin, D. S., Ochala, J., Domenighetti, A. A. & Fowler, V. M. Tropomodulin 1 directly controls thin filament length in both wild-type and tropomodulin 4-deficient skeletal muscle. *Development* **142**, 4351–4362 (2015).
  144. Fernandes, I. & Schöck, F. The nebulin repeat protein Lasp regulates I-band architecture and filament spacing in myofibrils. *The Journal of Cell Biology* **206**, 559–572 (2014).
  145. Shwartz, A., Dhanyasi, N., Schejter, E. D. & Shilo, B.-Z. The Drosophila formin Fhos is a primary mediator of sarcomeric thin-filament array assembly. *eLife* **5**, D786 (2016).
  146. Iskratsch, T. *et al.* Formin follows function: a muscle-specific isoform of FHOD3 is regulated by CK2 phosphorylation and promotes myofibril maintenance. *The Journal of Cell Biology* **191**, 1159–1172 (2010).
  147. Bang, M.-L. *et al.* Nebulin-deficient mice exhibit shorter thin filament lengths and reduced contractile function in skeletal muscle. *Journal of Cell Biology* **173**, 905–916 (2006).
  148. Pappas, C. T., Krieg, P. A. & Gregorio, C. C. Nebulin regulates actin filament lengths by a stabilization mechanism. *The Journal of Cell Biology* **189**, 859–870 (2010).
  149. Chu, M., Gregorio, C. C. & Pappas, C. T. Nebulin, a multi-functional giant. *Journal of Experimental Biology* **219**, 146–152 (2016).
  150. Zhou, Q. *et al.* Ablation of Cypher, a PDZ-LIM domain Z-line protein, causes a severe form of congenital myopathy. *Journal of Cell Biology* **155**, 605–612 (2001).
  151. White, R. B., Biérinx, A.-S., Gnocchi, V. F. & Zammit, P. S. Dynamics of muscle fibre growth during postnatal mouse development. *BMC Dev Biol* **10**, 21–11 (2010).
  152. Abmayr, S. M. & Pavlath, G. K. Myoblast fusion: lessons from flies and mice. *Development* **139**, 641–656 (2012).
  153. Snijders, T. *et al.* Satellite cells in human skeletal muscle plasticity. *Front Physiol* **6**, 283 (2015).
  154. Windner, S. E., Manhart, A., Brown, A., Mogilner, A. & Baylies, M. K. Nuclear Scaling Is Coordinated among Individual Nuclei in Multinucleated Muscle Fibers. *Developmental Cell* **49**, 48–62.e3 (2019).
  155. Demontis, F. & Perrimon, N. Integration of Insulin receptor/Foxo signaling and dMyc activity during muscle growth regulates body size in Drosophila. *Development* **136**, 983–993 (2009).
  156. Wang, S. *et al.* Mechanotransduction via the LINC complex regulates DNA replication in myonuclei. *The Journal of Cell Biology* **217**, 2005–2018 (2018).
  157. Metzger, T. *et al.* MAP and kinesin-dependent nuclear positioning is required for skeletal muscle function. *Nature* **484**, 120–124 (2012).
  158. Folker, E. S., Schulman, V. K. & Baylies, M. K. Muscle length and myonuclear position are independently regulated by distinct Dynein pathways. *Development* **139**, 3827–3837 (2012).
  159. Elhanany-Tamir, H. *et al.* Organelle positioning in muscles requires cooperation between two KASH proteins and microtubules. *The Journal of Cell Biology* **198**, 833–846 (2012).
  160. Wang, S., Reuveny, A. & Volk, T. Nesprin provides elastic properties to muscle nuclei by cooperating with spectraplakins and EB1. *The Journal of Cell Biology* **209**, 529–538 (2015).
  161. Roman, W. *et al.* Myofibril contraction and crosslinking drive nuclear movement to the periphery of skeletal muscle. *Nature cell biology* **19**, 1189–1201 (2017).

- 1  
2  
3  
4  
5  
6  
7  
8  
9  
10  
11  
12  
13  
14  
15  
16  
17  
18  
19  
20  
21  
22  
23  
24  
25  
26  
27  
28  
29  
30  
31  
32  
33  
34  
35  
36  
37  
38  
39  
40  
41  
42  
43  
44  
45  
46  
47  
48  
49  
50  
51  
52  
53  
54  
55  
56  
57  
58  
59  
60  
61  
62  
63  
64  
65
162. Roman, W. & Gomes, E. R. Nuclear positioning in skeletal muscle. *Semin. Cell Dev. Biol.* **82**, 51–56 (2018).
  163. Kaya-Copur, A. *et al.* The Hippo pathway controls myofibril assembly and muscle fiber growth by regulating sarcomeric gene expression. *eLife* **10**, (2021).
  164. Avellaneda, J. *et al.* Myofibril and mitochondria morphogenesis are coordinated by a mechanical feedback mechanism in muscle. *Nature Communications* 1–18 (2021). doi:10.1038/s41467-021-22058-7
  165. Pan, D. The hippo signaling pathway in development and cancer. *Developmental Cell* **19**, 491–505 (2010).
  166. Deng, H. *et al.* Spectrin regulates Hippo signaling by modulating cortical actomyosin activity. *eLife* **4**, e06567 (2015).
  167. Fletcher, G. C. *et al.* The Spectrin cytoskeleton regulates the Hippo signalling pathway. *The EMBO Journal* **34**, 940–954 (2015).
  168. Fletcher, G. C. *et al.* Mechanical strain regulates the Hippo pathway in Drosophila. *Development* **145**, dev159467–10 (2018).
  169. Soler, C., Han, J. & Taylor, M. V. The conserved transcription factor Mef2 has multiple roles in adult Drosophila musculature formation. *Development* **139**, 1270–1275 (2012).
  170. van den Heuvel, S. & Dyson, N. J. Conserved functions of the pRB and E2F families. *Nature Reviews Molecular Cell Biology* **9**, 713–724 (2008).
  171. Zappia, M. P. & Frolov, M. V. E2F function in muscle growth is necessary and sufficient for viability in Drosophila. *Nature Communications* **7**, 10509 (2016).
  172. Nikonova, E., Kao, S.-Y. & Spletter, M. L. Contributions of alternative splicing to muscle type development and function. 1–0 (2020). doi:10.1016/j.semcd.2020.02.003
  173. Oas, S. T., Bryantsev, A. L. & Cripps, R. M. Arrest is a regulator of fiber-specific alternative splicing in the indirect flight muscles of Drosophila. *The Journal of Cell Biology* **206**, 895–908 (2014).
  174. Swift, J. *et al.* Nuclear lamin-A scales with tissue stiffness and enhances matrix-directed differentiation. *Science* **341**, 1240104 (2013).
  175. Engler, A. J., Sen, S., Sweeney, H. L. & Discher, D. E. Matrix elasticity directs stem cell lineage specification. *CELL* **126**, 677–689 (2006).
  176. Shamipour, S., Caballero-Mancebo, S. & Heisenberg, C.-P. Cytoplasm's Got Moves. *Developmental Cell* **56**, 213–226 (2021).
  177. Denes, L. T., Kelley, C. P. & Wang, E. T. Microtubule-based Transport is Essential to Distribute RNA and Nascent Protein in Skeletal Muscle. *Nature Communications* **12**, 6079-19 (2021).
  178. Rudolph, F. *et al.* Resolving titin's lifecycle and the spatial organization of protein turnover in mouse cardiomyocytes. *Proceedings of the National Academy of Sciences* **112**, 201904385 (2019).
  179. Lewis, Y. E. *et al.* Localization of transcripts, translation, and degradation for spatiotemporal sarcomere maintenance. *J. Mol. Cell. Cardiol.* **116**, 16–28 (2018).
  180. Papadopoulos, S., Jürgens, K. D. & Gros, G. Protein diffusion in living skeletal muscle fibers: dependence on protein size, fiber type, and contraction. *Biophysj* **79**, 2084–2094 (2000).
  181. Wiedemann, N. & Pfanner, N. Mitochondrial Machineries for Protein Import and Assembly. *Annu. Rev. Biochem.* **86**, 685–714 (2017).
  182. Heinrich, L. *et al.* Automatic whole cell organelle segmentation in volumetric electron microscopy. *bioRxiv* 2020.11.14.382143 (2020). doi:10.1101/2020.11.14.382143

- 1  
2  
3  
4  
5  
6  
7  
8  
9  
10  
11  
12  
13  
14  
15  
16  
17  
18  
19  
20  
21  
22  
23  
24  
25  
26  
27  
28  
29  
30  
31  
32  
33  
34  
35  
36  
37  
38  
39  
40  
41  
42  
43  
44  
45  
46  
47  
48  
49  
50  
51  
52  
53  
54  
55  
56  
57  
58  
59  
60  
61  
62  
63  
64  
65
183. Bleck, C. K. E., Kim, Y., Willingham, T. B. & Glancy, B. Subcellular connectomic analyses of energy networks in striated muscle. *Nature Communications* **9**, 1–11 (2018).
  184. Mishra, P., Varuzhanyan, G., Pham, A. H. & Chan, D. C. Mitochondrial Dynamics is a Distinguishing Feature of Skeletal Muscle Fiber Types and Regulates Organellar Compartmentalization. *Cell Metabolism* **22**, 1033–1044 (2015).
  185. Glancy, B. *et al.* Mitochondrial reticulum for cellular energy distribution in muscle. *Nature* **523**, 617–620 (2015).
  186. Vincent, A. E. *et al.* Quantitative 3D Mapping of the Human Skeletal Muscle Mitochondrial Network. *CellReports* **26**, 996–1009.e4 (2019).
  187. Sauerwald, J., Backer, W., Matzat, T., Schnorrer, F. & Luschnig, S. Matrix metalloproteinase 1 modulates invasive behavior of tracheal branches during entry into *Drosophila* flight muscles. *eLife* **8**, 1079 (2019).
  188. Yim, A. *et al.* mitoXplorer, a visual data mining platform to systematically analyze and visualize mitochondrial expression dynamics and mutations. *Nucleic Acids Res.* **48**, 605–632 (2020).
  189. Zick, M., Rabl, R. & Reichert, A. S. Cristae formation-linking ultrastructure and function of mitochondria. *Biochim. Biophys. Acta* **1793**, 5–19 (2009).
  190. Cogliati, S. *et al.* Mitochondrial cristae shape determines respiratory chain supercomplexes assembly and respiratory efficiency. *CELL* **155**, 160–171 (2013).
  191. Porter, G. A. *et al.* Bioenergetics, mitochondria, and cardiac myocyte differentiation. *Prog Pediatr Cardiol* **31**, 75–81 (2011).
  192. Janota, C. S., Calero-Cuenca, F. J. & Gomes, E. R. The role of the cell nucleus in mechanotransduction. *Current opinion in cell biology* **63**, 204–211 (2020).
  193. Dorn, G. Mitochondrial fission/fusion and cardiomyopathy. *Current Opinion in Genetics & Development* **38**, 38–44 (2016).
  194. Favaro, G. *et al.* DRP1-mediated mitochondrial shape controls calcium homeostasis and muscle mass. *Nature Communications* **10**, 2576–17 (2019).
  195. Silva Ramos, E. *et al.* Mitochondrial fusion is required for regulation of mitochondrial DNA replication. *PLoS Genetics* **15**, e1008085 (2019).

1  
2  
3  
4  
5  
6  
7  
8  
9  
10  
11  
12  
13  
14  
15  
16  
17  
18  
19  
20  
21  
22  
23  
24  
25  
26  
27  
28  
29  
30  
31  
32  
33  
34  
35  
36  
37  
38  
39  
40  
41  
42  
43  
44  
45  
46  
47  
48  
49  
50  
51  
52  
53  
54  
55  
56  
57  
58  
59  
60  
61  
62  
63  
64  
65

**Box 1.**

**Sarcomere** - defined as the region flanked by two Z-discs with a M-band at its center. It is composed of bipolar myosin filaments intercalated with polar actin filaments. Sliding of actin filaments by pulling myosin motors results in sarcomere shortening.

**Myofibril** - a concatenation of sarcomeres that spans the length of a muscle fiber. Myofibrils form bundles which laterally align in cross-striated mammalian skeletal muscle or insect leg muscle. In fibrillar insect flight muscle, each myofibril is isolated from its neighbours by surrounding mitochondria.

**I-band** - or 'isotropic' band region, is the zone of the sarcomere without any myosin filaments. It spans across one Z-disc into to the adjacent sarcomere. When the muscle fiber contracts the I-band shortens.

**A-band** - or 'anisotropic' band region, is the region encompassing myosin bipolar filaments. Myosin filaments are cross-linked at the central M-band by M-band proteins, such as myomesin. A-band length is constant during sarcomere contraction.

**M-band** - the central part of the sarcomere composed of proteins that laterally cross-link the myosin filaments, likely providing rigidity and stability.

**Z-disc** - the connection between two sarcomeres. It is composed of several actin cross-linking proteins that stably anchor actin filaments at their plus ends. It also anchors the N-terminus of the gigantic titin protein.

**Titin** - the gigantic spring protein of the sarcomere. It connects actin to myosin filaments, by spanning in mammals from the Z-disc (titin N-terminus) to the M-band (titin C-terminus). It rules the length of the sarcomere, thus is shortens during sarcomere contraction.

1  
2  
3  
4  
5  
6  
7  
8  
9  
10  
11  
12  
13  
14  
15  
16  
17  
18  
19  
20  
21  
22  
23  
24  
25  
26  
27  
28  
29  
30  
31  
32  
33  
34  
35  
36  
37  
38  
39  
40  
41  
42  
43  
44  
45  
46  
47  
48  
49  
50  
51  
52  
53  
54  
55  
56  
57  
58  
59  
60  
61  
62  
63  
64  
65

1  
2  
3  
4  
5  
6  
7  
8  
9  
10  
11  
12  
13  
14  
15  
16  
17  
18  
19  
20  
21  
22  
23  
24  
25  
26  
27  
28  
29  
30  
31  
32  
33  
34  
35  
36  
37  
38

## Figure legends.

**Fig. 1. (A) The musculoskeletal system: a biomechanical apparatus.** The muscle fibers attach via tendons to two bones. Muscle contraction generates force to move the two skeletal elements closer together and thus powers body movement. **(B) The sarcomere: a force producing machine.** Scheme of the basic architecture of a vertebrate sarcomere with myosin filaments (blue) and actin filaments (red), which are stably linked by titin spanning from the Z-disc (dark green) to the M-band (light blue). Note that the myosin containing region is also called the A-band, whereas the myosin free actin region of the sarcomere is called the I-band. The scheme was modified from <sup>68</sup>. **(C) Titin: a molecular ruler.** Titin spans half the length of a vertebrate sarcomere providing a direct template for sarcomere length: PEVK spring domain deletions result in shorter sarcomeres with shorter I-bands, whereas deletions of titin A-band parts lead to shorter myosin filaments and thus shorter A-bands. **(D) Titin: a molecular spring and possible force sensor.** The elasticity of titin is generated by its Ig domain series and PEVK rich region, which extend and possibly unfold in relaxed muscle to store elastic energy. Upon contraction the domains compact or refold again elastically.

39  
40  
41  
42  
43  
44  
45  
46  
47  
48  
49  
50  
51  
52  
53  
54  
55  
56  
57  
58  
59  
60  
61  
62  
63  
64  
65

**Fig. 2. (A) Muscle-tendon attachment: a force resistant connection at molecular resolution. Top:** transmission electronic micrograph of a *Drosophila* flight muscle tendon cell connecting one flight muscle myofibril to the chitin exoskeleton (cuticle). Note the zig-zag pattern of the interface between tendon and muscle. Scale bar is 500 nm. **Bottom:** molecular scheme of a terminal Z-disc connecting to a tendon cell. A terminal integrin signalling mechanically connects via an actin-rich layer to the terminal Z-disc of a flight muscle myofibril. Scheme was inspired by <sup>94,103</sup>. **(B) Tension sensors: measuring molecular forces at muscle attachments.** A talin FRET-based tension sensor allows to quantify molecular forces across talin. The sensor is composed of a mechanosensitive peptide inserted between FRET

1 donor (D) and acceptor (A). Low tension results in a closed sensor and high FRET, while high  
2 force stretches the peptide and reduces FRET. Scheme was inspired by <sup>103</sup> and modified from  
3  
4 102.  
5  
6  
7  
8  
9

10 **Fig. 3. (A) *Drosophila* flight muscle morphogenesis.** Myotubes have attached to tendons at  
11 24 h APF and contain a cortical actomyosin network under lower tension. At 30 h APF tension  
12 has increased, myotubes have converted to myofibers and have assembled all their immature  
13 myofibrils into myofibril bundles. High tension produced long tendon extensions. After 30 h  
14 APF each myofibril and hence the entire myofiber grow in length and diameter resulting in a  
15 large muscle volume increase. Tendon extensions shrink. **(B) Myofibrillogenesis: sarcomere  
16 assembly and sarcomere maturation.** Schemes of actomyosin filament network without  
17 periodic patterns which assembles to long immature myofibrils containing periodic muscle  
18 myosin and titin. Each myofibril matures by isoform exchange and recruitment of more  
19 sarcomeric components to a mature sarcomere. **(C) Transcriptional dynamics recapitulates  
20 morphogenesis phases.** Complex transcriptional regulation patterns generate the necessary  
21 proteins at precise stages and sufficient quantities to the various muscle morphogenesis phases.  
22 Scheme was inspired by <sup>120</sup>.  
23  
24  
25  
26  
27  
28  
29  
30  
31  
32  
33  
34  
35  
36  
37  
38  
39  
40  
41  
42  
43

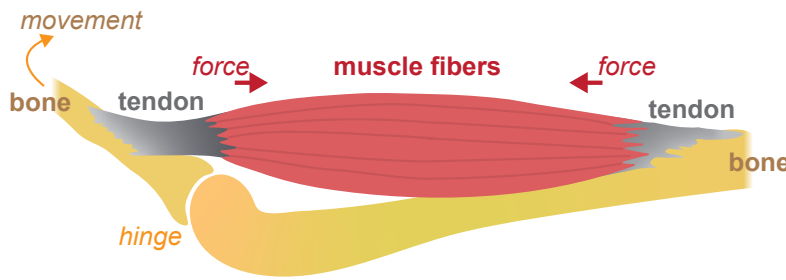
44 **Fig. 4. Muscle fibers: coordinating morphogenesis in a crowded space. Two examples of  
45 different mitochondria-myofibril architectures. Left:** Adult *Drosophila* fibrillar flight  
46 muscles contain round individual myofibrils (red) isolated from each other by large ellipsoid  
47 shaped mitochondria (green). Nuclei (blue) are located between the myofibril bundles. Note  
48 that myofibrils are squeezing mitochondria into their elongated shapes. **Right:** Mammalian  
49 skeletal muscle contain bundles of vertically aligned cross-striated myofibrils with  
50 mitochondria concentrated in groups squeezed in between. These mitochondria form long thin  
51  
52  
53  
54  
55  
56  
57  
58  
59  
60  
61  
62  
63  
64  
65

1 extensions along the sarcomeric I-bands that build networks. In both muscle types the crowded  
2 cellular environment generates mechanical pressure that positions the nuclei at the periphery  
3  
4 of myofibril bundles adopting an elongated shape.  
5  
6  
7  
8  
9  
10  
11  
12  
13  
14  
15  
16  
17  
18  
19  
20  
21  
22  
23  
24  
25  
26  
27  
28  
29  
30  
31  
32  
33  
34  
35  
36  
37  
38  
39  
40  
41  
42  
43  
44  
45  
46  
47  
48  
49  
50  
51  
52  
53  
54  
55  
56  
57  
58  
59  
60  
61  
62  
63  
64  
65



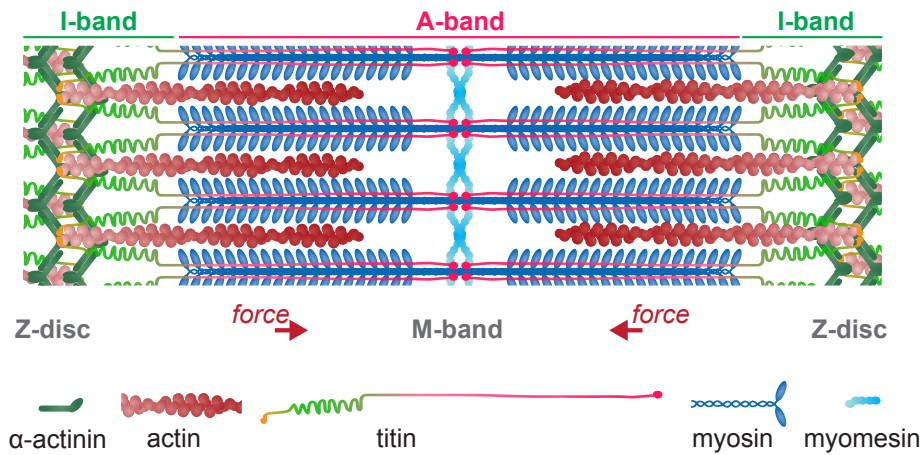
A

## the musculoskeletal system: a biomechanical apparatus



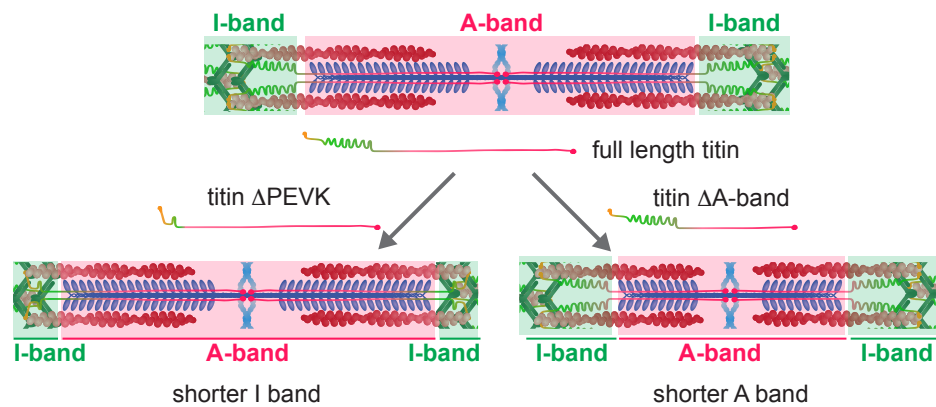
B

## the sarcomere: a force producing machine



C

## titin: a molecular ruler



D

## titin: a molecular spring and possible force sensor

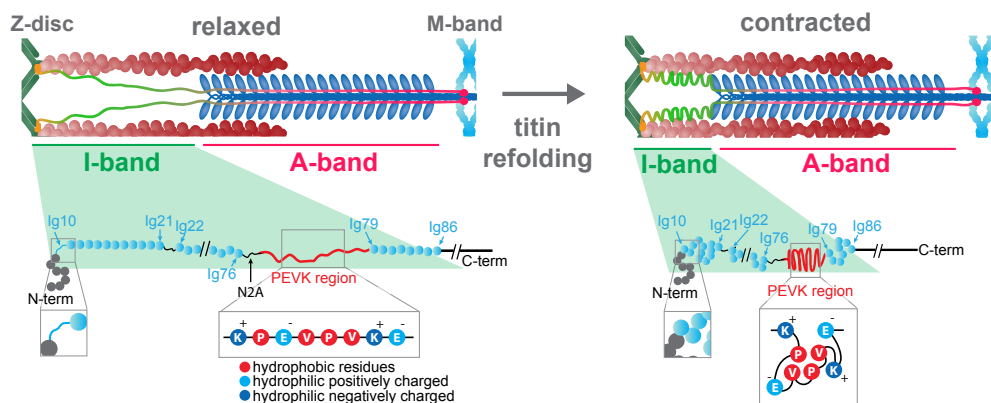
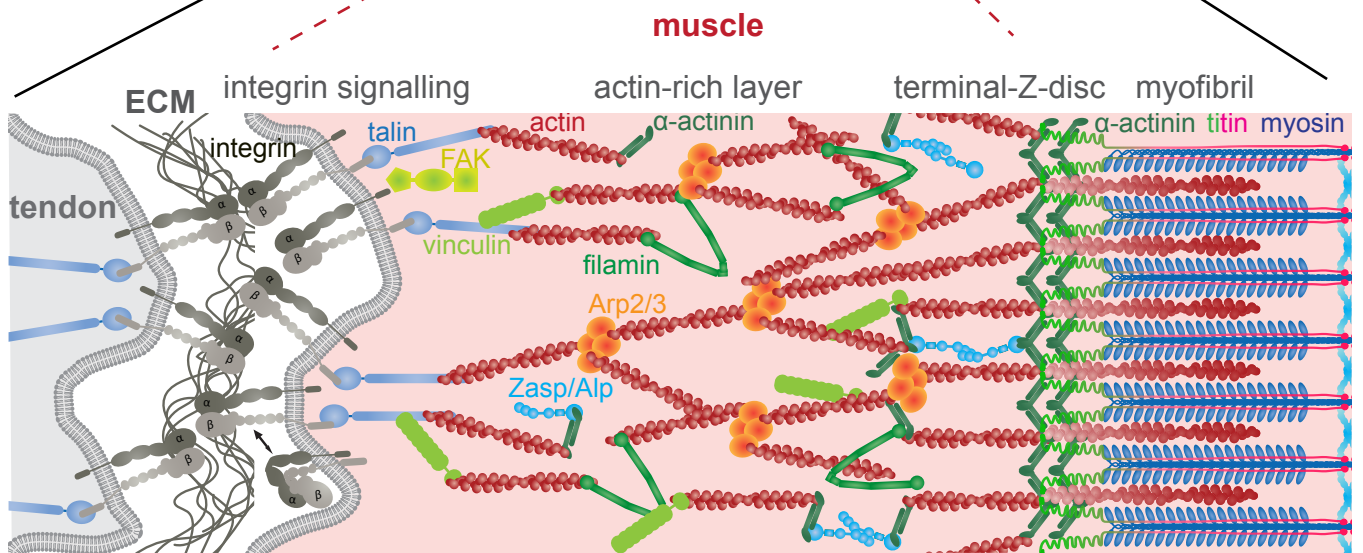
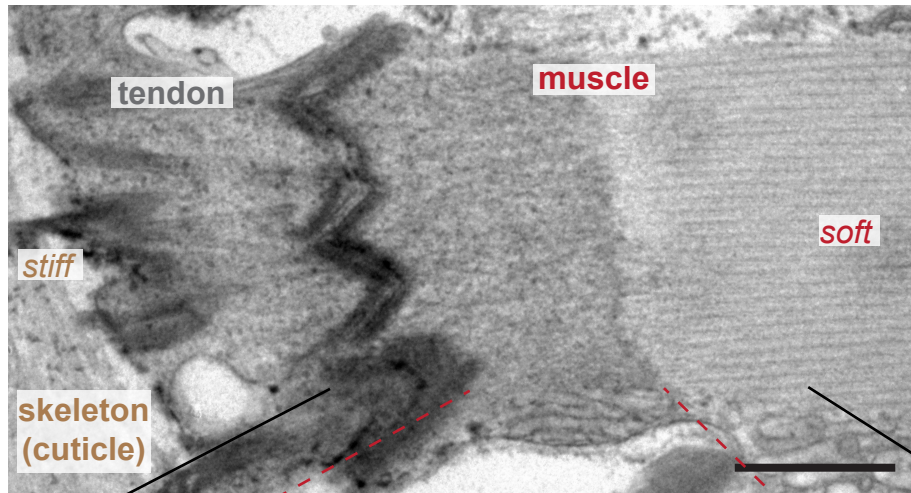


Figure 1

**A** muscle-tendon attachment:  
a force resistant connection at molecular resolution



**B** tension sensors:  
measuring molecular forces at muscle attachments

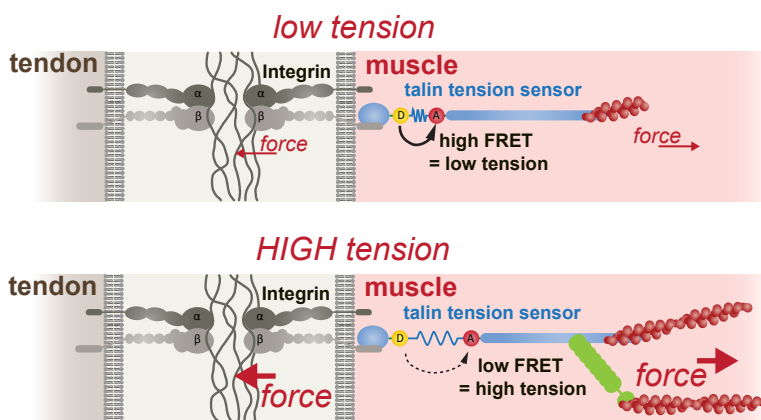
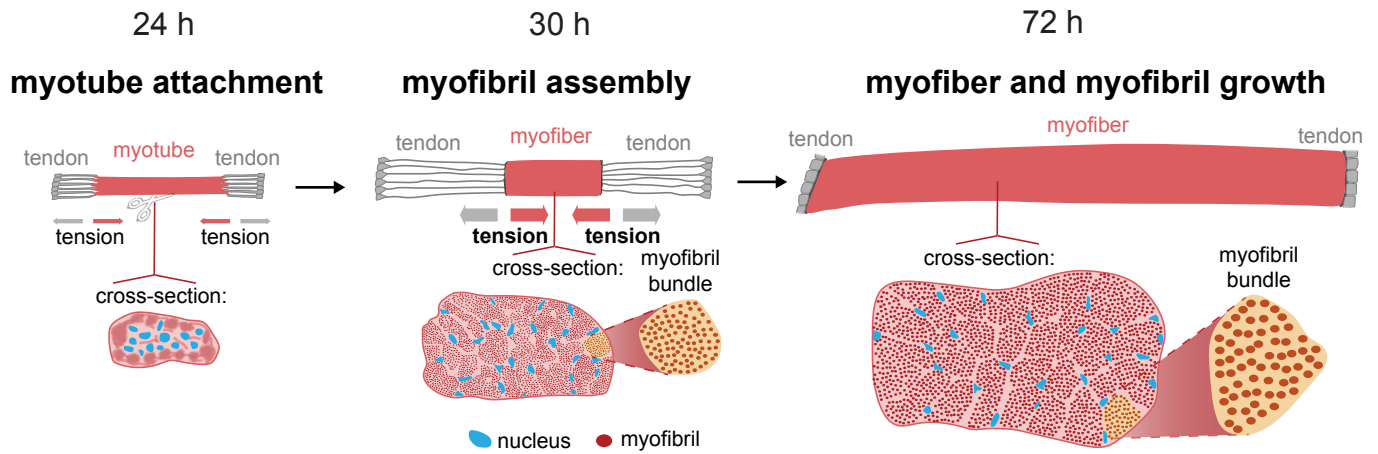
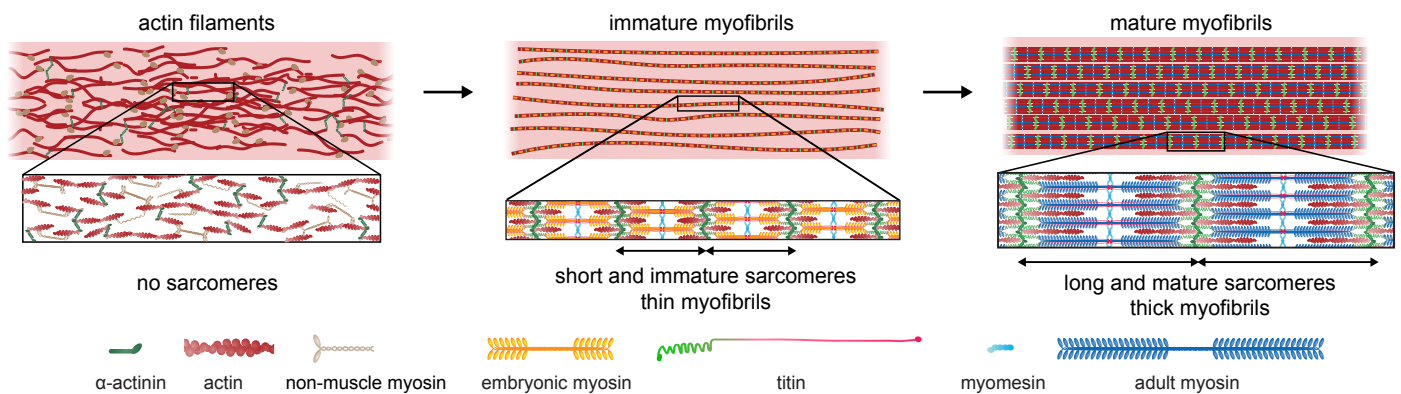


Figure 2

## A *Drosophila* flight muscle morphogenesis:



## B myofibrillogenesis: sarcomere assembly and sarcomere maturation



## C transcriptional dynamics recapitulates morphogenesis phases

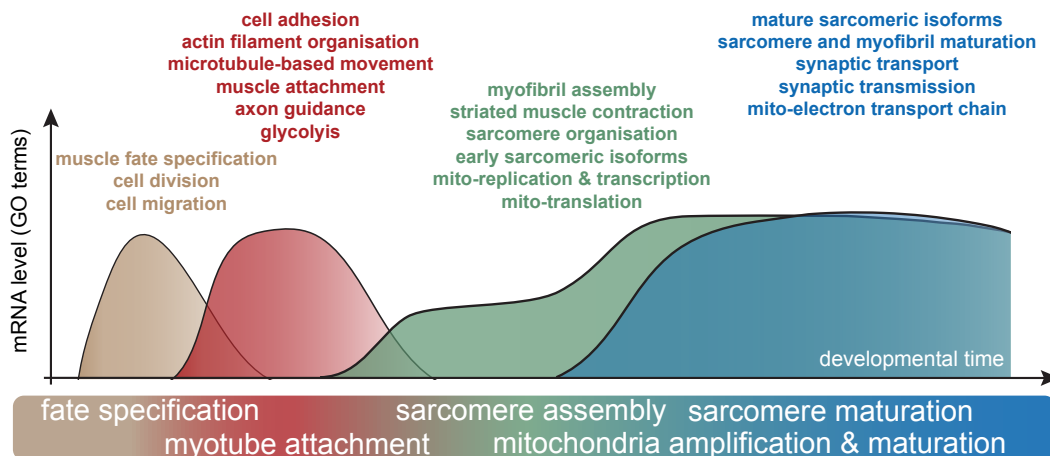


Figure 3

## muscle fibers: coordinating morphogenesis in a crowded space

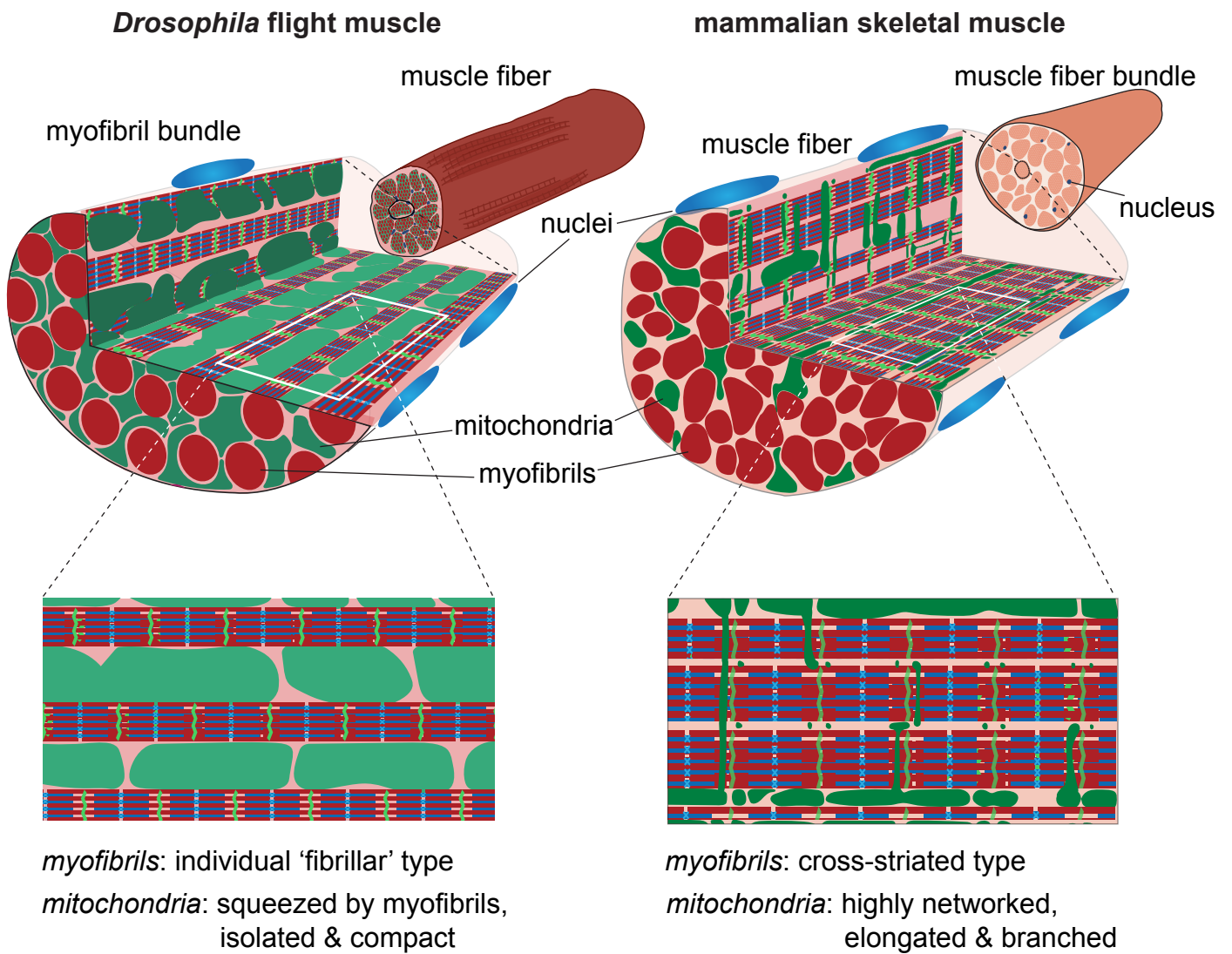


Figure 4

Nuno M Luis and Frank Schnorrer conceptualised the content, prepared the figures and drafted and revised the main text for this review together.